Eur. Phys. J. C 52, 999–1019 (2007)
DOI 10.1140/epjc/s10052-007-0434-0

THE EUROPEAN PHYSICAL JOURNAL C

Special Article – Scientific Note

Study of ATLAS sensitivity to FCNC top decays

The ATLAS Collaboration

J. Carvalho[1], N. Castro[1], L. Chikovani[2], T. Djobava[3], J. Dodd[4], S. McGrath[4], A. Onofre[1], J. Parsons[4], F. Veloso[1,a]

[1] LIP – Dep. Física, Universidade de Coimbra, 3004-516 Coimbra, Portugal
[2] E. Andronikashvili Institute of Physics, Tbilisi, Georgia
[3] High Energy Physics Institute, Tbilisi State University, Tbilisi, Georgia
[4] CU, Columbia University, Nevis Laboratories, 136 South Broadway, P.O. Box 137, Irvington, NY 10533, USA

Received: 29 March 2007 / Revised version: 13 September 2007 /
Published online: 16 October 2007 –

Abstract. The ATLAS experiment sensitivity to top quark flavour changing neutral current (FCNC) decays was studied at LHC using $t\bar{t}$ events. While one of the top quarks is expected to follow the dominant Standard Model decay $t \to bW$, the other decays through a FCNC channel, i.e. $t \to Zu(c)$, $t \to \gamma u(c)$ or $t \to gu(c)$. Different types of analyses, applied to each FCNC decay mode, were compared. The FCNC branching ratio sensitivity (assuming a 5σ signal significance) and 95% confidence level limits on the branching ratios (in the hypothesis of signal absence) were obtained.

1 Introduction

Flavour changing neutral currents (FCNC) are strongly suppressed in the standard model (SM) due to the Glashow–Iliopoulos–Maiani (GIM) mechanism [1]. Although absent at tree level, small FCNC contributions are expected at one loop level, according to the Cabibbo–Kobayashi–Maskawa (CKM) mixing matrix [2–5]. In the top quark sector of the SM, these contributions limit the FCNC decay branching ratios to the gauge bosons, $\mathrm{BR}_{t\to qX}$ $(X = Z, \gamma, g)$, to below 10^{-10}. There are however extensions of the SM, like supersymmetry (SUSY) [6], multi-Higgs doublet models [7] and SM extensions with exotic (vector-like) quarks [8], which predict the presence of FCNC contributions already at tree level and significantly enhance the FCNC decay branching ratios compared to the SM predictions.

Due to its large mass, much higher than any other known fermion, the top quark is a very good laboratory to look for physics beyond the SM. If the top quark has FCNC anomalous couplings to the gauge bosons, its decay properties would be affected, and possibly measured at colliders, in addition to the dominant decay mode $t \to bW$. Indeed one of the most prominent signatures of FCNC processes at the large hadron collider (LHC), would be the direct observation of a top quark decaying into a charm or an up quark together with a γ, g or Z boson [9]. In the effective Lagrangian approach [10, 11] the new top quark decay rates to the gauge bosons [12],

$$\Gamma(t \to qg) = \left(\frac{\kappa_{tq}^{g}}{\Lambda}\right)^2 \frac{8}{3}\alpha_{\mathrm{s}} m_t^3 \,, \tag{1}$$

$$\Gamma(t \to q\gamma) = \left(\frac{\kappa_{tq}^{\gamma}}{\Lambda}\right)^2 2\alpha m_t^3 \,, \tag{2}$$

$$\Gamma(t \to qZ)_{\gamma} = \left(\left|v_{tq}^{Z}\right|^2 + \left|a_{tq}^{Z}\right|^2\right) \alpha m_t^3 \frac{1}{4M_Z^2 \sin^2 2\theta_W} \times \left(1 - \frac{m_Z^2}{m_t^2}\right)^2 \left(1 + 2\frac{m_Z^2}{m_t^2}\right) \text{ and} \tag{3}$$

$$\Gamma(t \to qZ)_{\sigma} = \left(\frac{\kappa_{tq}^{Z}}{\Lambda}\right)^2 \alpha\, m_t^3 \frac{1}{\sin^2 2\theta_W} \times \left(1 - \frac{m_Z^2}{m_t^2}\right)^2 \left(2 + \frac{m_Z^2}{m_t^2}\right), \tag{4}$$

can be expressed in terms of the κ_{tq}^{g}, κ_{tq}^{γ}, $(|v_{tq}^{Z}|^2 + |a_{tq}^{Z}|^2)$ and κ_{tq}^{Z} anomalous couplings to the g, γ and Z bosons respectively. The energy scale associated with this new physics is represented by Λ, while α_{s} and α are, respectively, the strong and electromagnetic coupling constants. The electroweak mixing angle is represented by θ_W and the top and Z masses are represented, respectively, by m_t and m_Z.

Although FCNC processes associated with the production [13–16] and decay[17] of top quarks have been studied at colliders ($\mathrm{BR}_{t\to Zq} < 33\%$ and $\mathrm{BR}_{t\to\gamma q} < 3.2\%$ at 95% confidence level (CL) [17]), the amount of top quark

[a] e-mail: filipe.veloso@lipc.fis.uc.pt

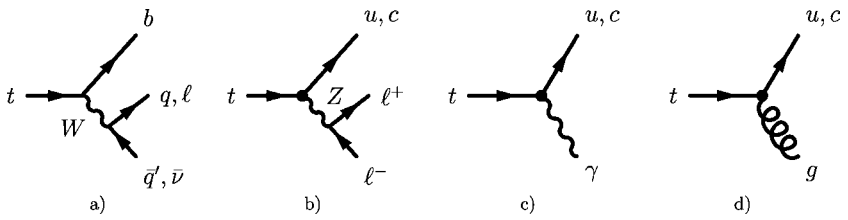

Fig. 1. Feynman diagrams for the top quark decays considered in this paper: **a** SM decay $t \to bW$; **b** FCNC decay $t \to Zq$; **c** FCNC decay $t \to \gamma q$ and **d** FCNC decay $t \to gq$

relevant data collected up to now is not comparable with the statistics expected at the LHC. The LHC will operate with a centre-of-mass energy of 14 TeV, and in the low luminosity phase ($l = 10^{33}\,\mathrm{cm}^{-2}\,\mathrm{s}^{-1}$), several millions of top quarks will be produced per year and experiment, mainly in pairs (with a NLO cross-section of 833 pb [12, 18, 19]), but also through single top production (with an expected NLO cross-section of 280 pb [20, 21]).

This paper is devoted to the study of the ATLAS experiment [22] sensitivity to FCNC top quark decays at the LHC. While one of the top quarks is expected to follow the dominant SM decay ($t \to bW$), the other decays through a FCNC channel, i.e. $t \to Zq$, $t \to \gamma q$ or $t \to gq$. The corresponding Feynman diagrams are shown in Fig. 1. Different types of analyses (cut-based and likelihood-based) were applied to each FCNC decay mode and their results compared.

This paper is organised as follows. After the introduction, a description of the simulated signal and background is given in Sect. 2. The analysis criteria applied to each FCNC channel are described in Sect. 3 and in Sect. 4 a comparison of the results obtained by the different analyses [23, 24] is presented within two different approaches: branching ratio sensitivities (assuming a 5σ signal significance for discovery) and 95% confidence level limits (in the hypothesis of signal absence). These results are compared with previously published ones [13–17, 22, 25, 26]. In Sect. 5 the conclusions are presented.

2 Signal and background simulation

The Monte Carlo (MC) generation of the QCD ($b\bar{b}$), $W+$ jets, Z/γ^*+jets, WW, ZZ and ZW background processes was done with the library PYTHIA [27]. Single top quark production was generated with TopReX 4.05 [28], and the SM top pair production ($t\bar{t}_{\mathrm{SM}}$) was generated using TopReX and PYTHIA. These libraries were also used to generate signal $t\bar{t}$ samples, where one of the t-quarks decays via charged currents (CC) into bW and the other one decays through FCNC into qZ, $q\gamma$ or qg. For TopReX the anomalous couplings to the g, γ and Z bosons were set to $\kappa^g_{tq} = \kappa^\gamma_{tq} = (|v^Z_{tq}|^2 + |a^Z_{tq}|^2)^{1/2} = \kappa^Z_{tq} = 0.1$ and Λ was set to 1 TeV. The top mass was set to $175\,\mathrm{GeV}/c^2$. Different values, $170\,\mathrm{GeV}/c^2$ and $180\,\mathrm{GeV}/c^2$, were also considered for the study of systematic uncertainties, as explained in Sect. 4.3. No SUSY backgrounds or other contributions beyond the SM were considered in the present analyses. The CTEQ2L and CTEQ5L parton distribution functions (PDF) were used [27, 28] in the analyses and the CTEQ4M was used for systematic studies. No pile-up was taken into account.

The generated background and signal events were passed through the ATLAS fast simulation packages ATLFAST [29] and ATLFASTB [29]. For each event, these packages begin by simulating the energy deposition in the calorimeter cells of all the stable particles. The calorimeter cells are clustered within a cone of $\Delta R = \sqrt{(\Delta\phi)^2 + (\Delta\eta)^2} = 0.4$. Cells with $E_{\mathrm{T}} > 1.5\,\mathrm{GeV}$ are used as cluster seeds and the cone algorithm is applied in decreasing order of E_{T}. Only clusters with $E_{\mathrm{T}} > 5\,\mathrm{GeV}$ are considered. The polar angle and the momentum of photons are smeared according to Gaussian parameterizations. For electrons, their momenta are smeared according to a Gaussian parameterizations. The momentum of each muon is smeared according to a resolution which depends on the p_{T}, $|\eta|$ and ϕ. The photon (electron) energy resolution is $\delta E/E < 2.9\%$ (3.3%), for $E > 20\,\mathrm{GeV}$. The transverse momentum resolution of muons with $p_{\mathrm{T}} < 100\,\mathrm{GeV/c}$ is $\delta p_{\mathrm{T}}/p_{\mathrm{T}} \lesssim 2\%$. Photons, electrons and muons are selected only if they have $|\eta| < 2.5$ and $p_{\mathrm{T}} > 5\,\mathrm{GeV}/c$ ($p_{\mathrm{T}} > 6\,\mathrm{GeV}/c$ for muons). They are classified as isolated if the transverse energy of the cluster associated to the particle, inside a cone of $\Delta R = 0.2$, does not exceed 10 GeV the particle energy, and the ΔR from other energy clusters must be above 0.4. The clusters of energy depositions not associated to isolated photon, electrons or muons are used for the jet reconstruction. Their momenta are smeared according to a Gaussian distribution which depends on $|\eta|$. Jets are selected if they have $E_{\mathrm{T}} > 10\,\mathrm{GeV}$. For $E > 20\,\mathrm{GeV}$, the jet energy resolution is less than 12% ($|\eta| < 3$) and less than 24% ($|\eta| > 3$). The missing transverse momentum is estimated by summing the transverse momentum of the isolated photons, electrons, muons and jets. The non isolated muons and the clusters of energy deposition not associated to isolated photons, electrons, muons or jets, are also taken into account. In the ATLAS detector, it will be possible to identify b-jets with $|\eta| < 2.5$ by using b-tagging tools. The algorithm was simulated by setting a b-tagging efficiency to 60%, with contamination factors set to 14.9% (1.1%) for c-jets (light quark, gluon and tau jets) for the low luminosity phase ($l = 10^{33}\,\mathrm{cm}^{-2}\,\mathrm{s}^{-1}$). In order to check the dependence of the analysis with the b-tagging efficiencies, different values, 50% and 70% (corresponding to the expected b-tag variation within the interesting signal transverse momentum range), were also considered for the systematic studies and the high luminosity phase ($l = 10^{34}\,\mathrm{cm}^{-2}\,\mathrm{s}^{-1}$), with contamination factors of 9.2% (0.4%) and 23.3% (2.9%) for c-jets (light quark, gluon and tau jets), respectively.

Initial and final state QED and QCD radiation (ISR + FSR), multiple interactions and hadronization were taken into account in the event generation. Due to the hadronization and FSR, the jets are reconstructed with less energies than those from the original quarks or gluons. The jets energies were calibrated by the ATLFASTB package, by applying a calibration factor, $K^{\rm jet} = p_{\rm T}^{\rm parton}/p_{\rm T}^{\rm jet}$, that is the ratio between the true parton energy and the reconstructed jet energy. The calibration factor depends on the $p_{\rm T}$ and is different for b-tagged and light jets.

Preliminary full simulation studies, based on the ATHENA framework [30], indicate a fair agreement between the fast and full simulations of the ATLAS detector.

3 Topologies and event selection

The $t\bar{t}$ final states corresponding to the different FCNC top decay modes lead to different topologies according to the number of jets, leptons and photons. There is however a common characteristic of all channels under study, i.e. in all of them one of the top quarks is assumed to decay through the dominant SM decay mode $t \to bW$ and the other is forced to decay via one of the FCNC modes $t \to Zq$, $t \to \gamma q$ or $t \to gq$. Two different types of analyses, labelled "cut-based" and "likelihood-based", were used to study the ATLAS sensitivity to FCNC top quark decays. For both analyses the leptonic decays of the W ($W \to \ell\nu_\ell$) were taken into account.[1] In addition, for the FCNC channel $t \to Zq$, the hadronic decay of the W ($W \to qq'$) was also considered for the cut-based analysis.

3.1 $t \to Zq$ channel

The QCD backgrounds at hadron colliders make the search for the signal via the fully hadronic channel (when both the W and Z decay hadronically) very difficult. For this reason only the leptonic decay of the Z was considered. The final state was then determined by the decays of the W boson. Two different possible decay channels have been considered: the first ('leptonic mode') where the W decays leptonically $W \to \ell\nu$, and the second ('hadronic mode') with $W \to jj$. The hadronic W decay signature has a larger branching fraction, but suffers from larger backgrounds. The experimental signature of the leptonic mode includes three isolated charged leptons, two of which reconstruct a Z boson, large missing transverse energy due to the neutrino and at least two jets, one of which is tagged as a b-jet. The signature of the hadronic mode is characterised by having two leptons (again with $m_{\ell^+\ell^-} \approx m_Z$) and at least four jets, one of which is tagged as a b-jet. Following a previous analysis [25], new cut-based [23] and likelihood-based [24] analyses were developed and are described below.

[1] For the cut-based analyses $\ell = e, \mu$, while for the likelihood-based analyses $\ell = e, \mu, \tau$

3.1.1 Cut-based analysis: hadronic mode

The final state for the hadronic W decay mode is $t\bar{t} \to ZqWb \to \ell^+\ell^- jjjb$. This mode has the following backgrounds: $Z+$jets production, followed by the decay $Z \to \ell^+\ell^-$, $pp \to W^\pm Z + X \to jj\ell^+\ell^- + X$, and $t\bar{t} \to WbWb$ with the final state topologies (a) $\ell^+\nu b\ell^-\bar{\nu}b$, or (b) $\ell^\pm\nu bjjb$. In the case of (a), the additional two jets must come from QCD radiation, while in (b) the source of leptons is from cascade decays. $Z+$jets production at the LHC has a relatively large cross-section, dominated by $qg \to Zq$ and $q\bar{q} \to Zg$ processes. To decrease the size of the background sample which needed to be generated, thresholds were imposed at the generator level on the invariant mass, $m = \sqrt{\hat{s}} > 130\ {\rm GeV}/c^2$, where $\sqrt{\hat{s}}$ is the effective centre-of-mass energy, and transverse momentum, $p_{\rm T} > 50\ {\rm GeV}/c$, of the hard scattering process. The cross-section for this subsample of events was $\sigma_{Z+{\rm jets}} = 3186$ pb. The WZ background is the electroweak process $pp \to W^\pm Z + X$, and has an assumed cross-section of $\sigma_{WZ} = 26.58$ pb. Background samples of 2.1×10^7 $Z+$jets events, 1.2×10^5 WZ events and $2.8 \times 10^7 t\bar{t}$ events were generated. Assuming the above mentioned production cross-sections, and including the relevant branching ratios, these background samples correspond to an integrated luminosity of $100\ {\rm fb}^{-1}$.

The analysis began with preselection cuts requiring that the event contains at least two charged leptons (electrons with $p_{\rm T} > 5\ {\rm GeV}/c$ within pseudorapidity $|\eta| < 2.5$ and muons with $p_{\rm T} > 6\ {\rm GeV}/c$ within pseudorapidity $|\eta| < 2.4$), and include a pair of opposite-sign and same-flavour leptons, compatible with them having come from a Z decay. In addition, the number of jets with $p_{\rm T_{jet}} > 15\ {\rm GeV}/c$ within pseudorapidity $|\eta| < 5.0$ was required to be at least four. After preselection cuts, 46% of the signal events were accepted, while only 3.0%, 3.5% and 4.1% of the $t\bar{t}$, $Z+$jets and WZ background events, respectively, were selected.

The next cuts required the presence of two isolated leptons with $p_{{\rm T}\ell} > 20\ {\rm GeV}/c$ and the demand for at least four jets with $p_{\rm T_{jet}} > 50\ {\rm GeV}/c$ and $|\eta^j| < 2.5$. The isolation ΔR of the jets (measured in relation to other jets and leptons) was then required to be greater than 0.4.

Figure 2 presents the distributions of reconstructed dilepton invariant mass and of reconstructed $t \to Zq$ invariant mass $m_{\ell\ell j}$ for the best combinations of $\ell\ell j$ (i.e. $\ell\ell j$ combination with the closest to top mass value of invariant mass $m_{\ell\ell j}$) for the signal sample. A cut was then applied on the dilepton invariant mass, requiring that it lie within $\pm 6\ {\rm GeV}/c^2$ around m_Z.

To suppress the large remaining $Z+$jets background, it was necessary to use the information that signal events contain, in addition to the decay $t \to Zq$, a hadronic decay $t \to Wb \to jjb$ of the other top quark. The hadronic top quark decay was, therefore, reconstructed as part of the signal requirement. First, a pair of jets was required to have an invariant mass m_{jj} within a $16\ {\rm GeV}/c^2$ around m_W. Figure 3 shows the distribution of reconstructed m_{jj} for the best combinations of jj (i.e. jj combination with the closest to W mass value of invariant mass m_{jj}) for the signal events. The W mass resolution is $\sigma_{m_{jj}} = 8\ {\rm GeV}/c^2$. A requirement was then made to have exactly one jet

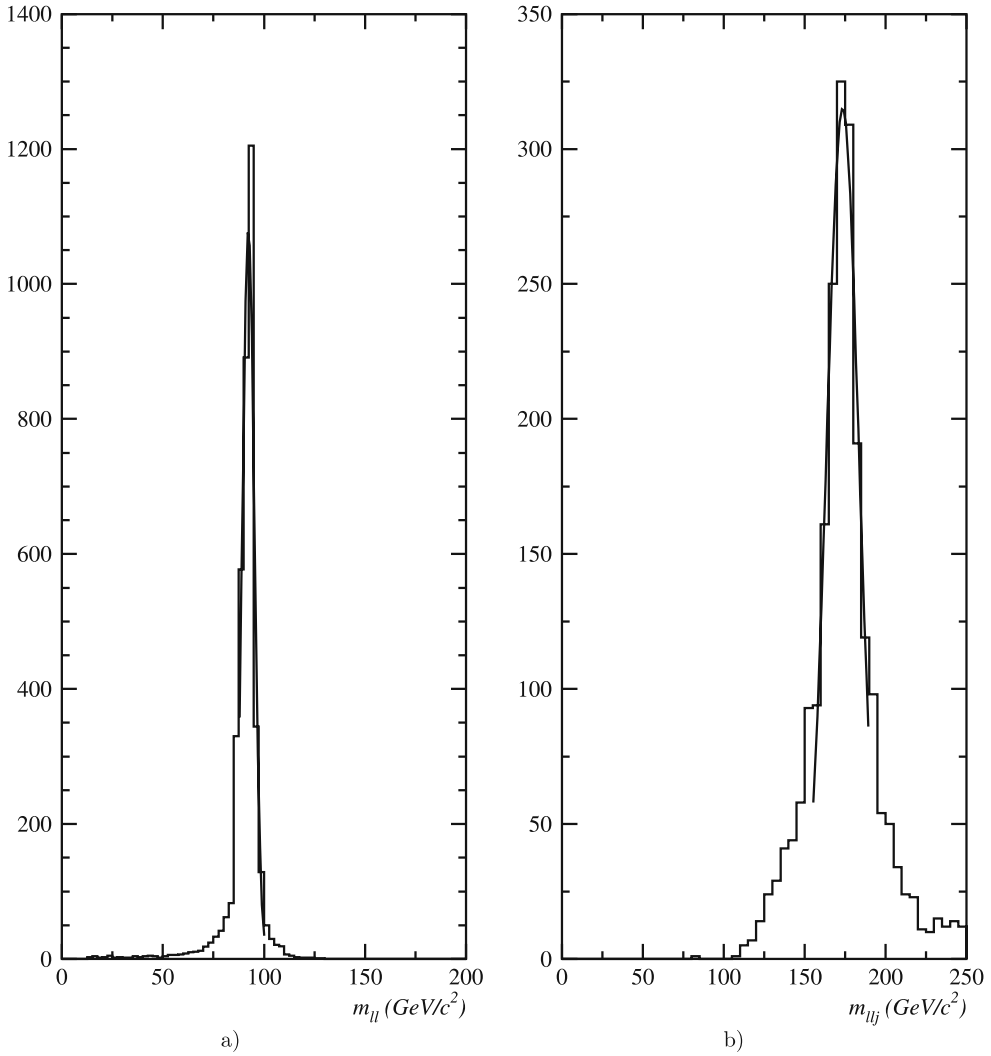

Fig. 2. Distributions for the hadronic mode of **a** reconstructed invariant mass of the lepton pairs, $m_{\ell\ell}$ for the best combination and **b** reconstructed invariant mass of $t \to \ell\ell j$ for the best combination of llj

tagged as a b-jet. Finally,the jjb invariant mass was required to lie within 8 GeV/c^2 around m_t.

Figure 3 presents the distribution of the reconstructed invariant top mass (m_{jjb}) for the best combinations of jjb (i.e. jjb combination with the closest to top mass value of invariant mass m_{jjb}) for the signal. The top mass resolution is $\sigma(m_{jjb}) = 18.5\,\mathrm{GeV}/c^2$, implying that the mass window applied is rather narrow in order to get a large background rejection. The sequence of cuts required to reconstruct the hadronic decay of the other top quark dramatically suppresses the backgrounds, but also reduces the signal efficiency by almost an order of magnitude. For those events with an accepted $t \to jjb$ candidate, the invariant mass of the Z candidate with the remaining unassigned high p_{T} jets was reconstructed to look for a signal from $t \to Zq$ decays. The resolution σ of $m_{\ell\ell j}$ distribution is $\sigma_{m_{\ell\ell j}} = 9.9\,\mathrm{GeV}/c^2$ (see Fig. 2). The analysis cuts reduce the WZ background to a negligible level in the $m_{Zq} \pm 24\,\mathrm{GeV}/c^2$ mass window. Two events of the $Z+$jets background are accepted in this mass window.

Table 1 summarises the effects of the sequential application of the above described various analysis cuts on the background samples and on the sample of 19 000 signal events of the topology $t\bar{t} \to ZqWb \to \ell^+\ell^- jjjb$.

3.1.2 Cut-based analysis: leptonic mode

The final state for the leptonic decay mode is $t\bar{t} \to ZqWb \to \ell^+\ell^- j\ell\nu b$. The experimental signature therefore includes three isolated charged leptons, two of which reconstruct a Z boson, and large missing transverse energy due to the undetected neutrino.

This mode has the following backgrounds: $Z(\to \ell\ell)+$ jets, $pp \to W^{\pm}Z + X \to \ell^{\pm}\nu\ell^+\ell^- + X$, and $t\bar{t} \to W^+bW^-\bar{b} \to \ell^+\nu b\ell^-\bar{\nu}b$. Assuming the production cross-sections given earlier, and including the relevant branching ratios, background samples of 2.1×10^7 $Z+$jets events, 38 000 WZ events, and 3.9×10^6 $t\bar{t}$ events were generated. These background samples correspond to an integrated luminosity of 100 fb^{-1}.

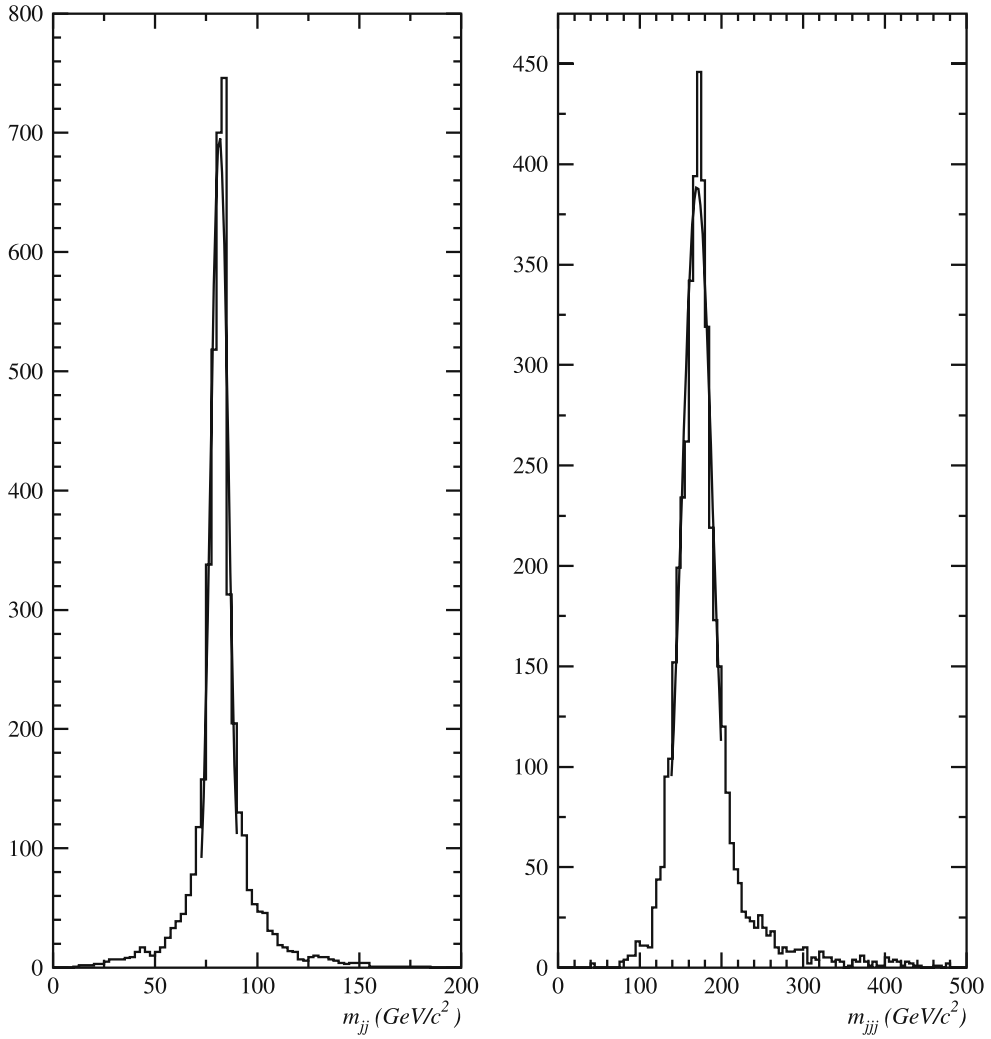

Fig. 3. Distributions for the hadronic mode of **a** reconstructed invariant mass of the jet pairs, m_{jj} for the best combination and **b** reconstructed invariant mass of $t \to jjb$ for the best combination of jjb

Table 1. The number of events, normalised to $L = 100\,\mathrm{fb}^{-1}$, and efficiency (%) of selection cuts applied in sequence for the signal and backgrounds in the hadronic decay mode in the $t \to Zq$ channel, obtained with a cut-based analysis, are shown

Description of cuts	Signal $t \to Zq$	Background processes Z+jets	$Z + W$	$t\bar{t}$ di-leptonic	$t\bar{t}$ semi-leptonic
	ε (%)	Nevt	Nevt	Nevt	Nevt
Preselection (2 leptons, 4 jets)	46.0	7.5×10^5	4970	5.8×10^5	2.7×10^5
2 leptons, $p_{\mathrm{T}}^{\ell} > 20\,\mathrm{GeV}/c$	37.7	5.9×10^5	4456	428 800	11 200
4 jets, $P_{\mathrm{T}}^{\mathrm{jet}} > 50\,\mathrm{GeV}/c$	15.2	63 478	400	35 530	870
$\Delta R_{jj} > 0.4$	14.9	60 421	390	35 370	830
$\Delta R_{lj} > 0.4$	14.9	60 394	361	35 370	830
$m_Z \pm 6\,\mathrm{GeV}$	12.8	50 973	268	3104	60
$m_W \pm 16\,\mathrm{GeV}$	5.3	14 170	139	719	37
one b-tag	2.2	1379	11	376	15
$m_{Wb} = m_t \pm 8\,\mathrm{GeV}$	0.6	90	1	28	4
$m_{Zq} = m_t \pm 24\,\mathrm{GeV}$	0.4	2	0	5	0

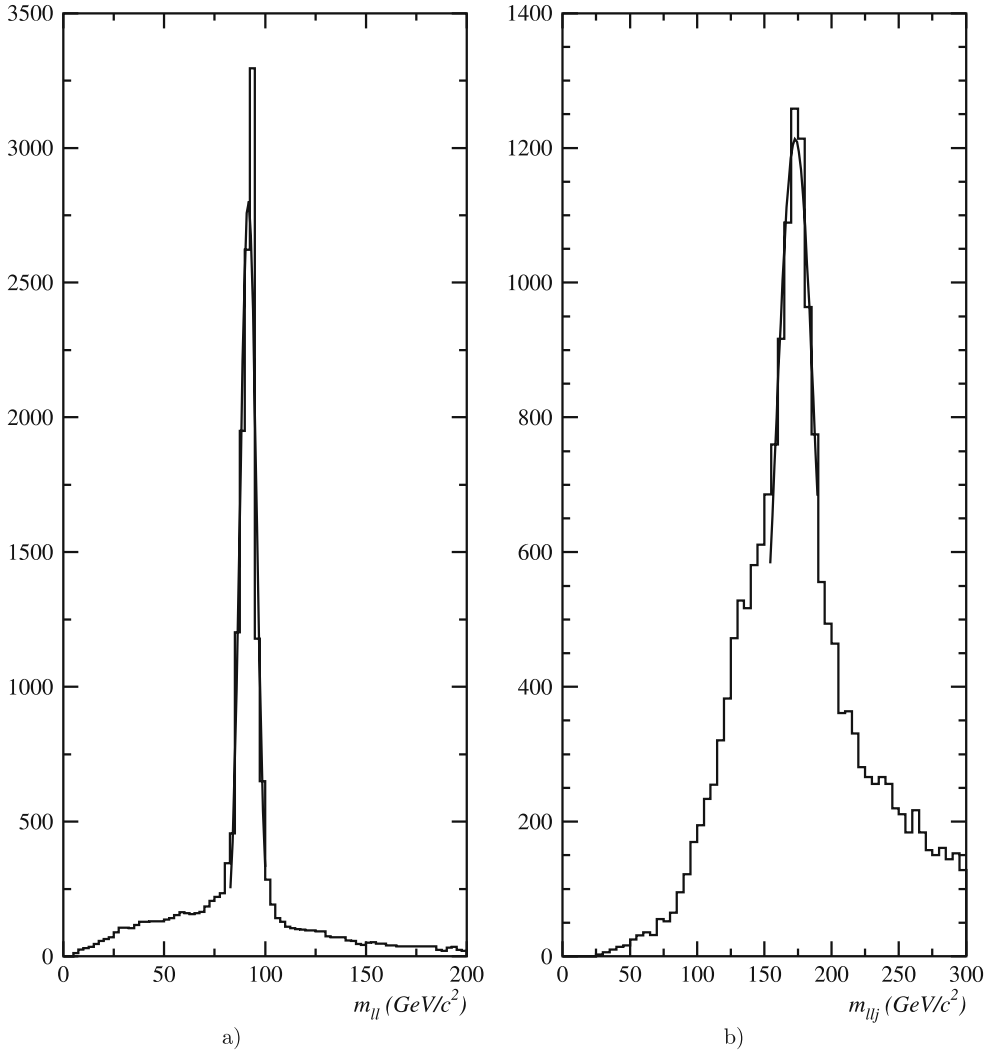

Fig. 4. Distributions for the leptonic mode of **a** reconstructed invariant mass of the lepton pairs, $m_{\ell\ell}$ and **b** reconstructed invariant mass of $t \to Zq \to \ell\ell j$

Preselection cuts were first applied, requiring the presence of at least three charged leptons (electrons with $p_{\mathrm{T}} > 5\,\mathrm{GeV}/c$ and muons with $p_{\mathrm{T}} > 6\,\mathrm{GeV}/c$) within pseudorapidity $|\eta| < 2.5$. Of these, at least one pair of leptons must be of opposite sign and same flavour, compatible with them being produced from a Z decay. In addition, the number of jets in the event with $p_{\mathrm{T_{jet}}} > 15\,\mathrm{GeV}/c$ within pseudorapidity $|\eta| < 5.0$ was required to be at least two. The requirement of three leptons reduces significantly the $Z+$jets and $t\bar{t}$ backgrounds, while the requirement of two jets reduces significantly WZ and $Z+$jets backgrounds.

The lepton criteria were then tightened, by requiring the presence of at least three isolated, charged leptons (electrons or muons) with $p_{\mathrm{T}\ell} > 20\,\mathrm{GeV}/c$. The next requirement, namely that the missing transverse momentum in the event satisfies $\not{p}_{\mathrm{T}} > 30\,\mathrm{GeV}/c$, is effective at further reducing the $Z+$ jets background while having little impact on the signal and other background sources. Next, it was demanded that there be at least two jets with $p_{\mathrm{T_{jet}}} > 50\,\mathrm{GeV}/c$, $|\eta_{\mathrm{jet}}| < 2.5$, and satisfying the following isolation conditions: $\Delta R_{jj} > 0.4$ (jet–jet isolation) and $\Delta R_{\ell j} > 0.4$ (lepton–jet isolation). The cut requiring the presence of two or more jets in each event effectively suppresses the WZ background.

The presence of a reconstructed $Z \to \ell^+\ell^-$ decay is a powerful cut against the $t\bar{t}$ background. A like-sign, same-flavor pair of isolated leptons was required to reconstruct to the Z mass within $m_Z \pm 6\,\mathrm{GeV}/c^2$. Figure 4 presents the distribution of reconstructed invariant mass of $\ell\ell$ pairs $m_{\ell\ell}$, for all dilepton combinations for the signal events. The width of the accepted window corresponds to approximately twice the Z mass resolution of about $2.9\,\mathrm{GeV}/c^2$. The next requirement was the presence in the event of exactly one tagged b-jet, which is effective at further reducing the WZ background. Finally, a peak at the top quark mass in the Zj invariant mass distribution was sought. In Fig. 4, the distribution of reconstructed invariant mass $m_{\ell\ell j}$ for all combinations of $\ell\ell j$ is presented for the signal events. The top quark mass resolution

Table 2. The number of events, normalised to $L = 100\,\text{fb}^{-1}$, and efficiency (%) of selection cuts applied in sequence for the signal and backgrounds for the leptonic mode in the $t \to Zq$ channel, obtained with a cut-based analysis, are shown

Description of cuts	Signal $t \to Zq$ ε (%)	Background processes Z+jets Nevt	$Z+W$ Nevt	$t\bar{t}$ Nevt
Preselection (3 leptons, 2 jets)	80.2	3.7×10^5	2941	11.7×10^5
3 leptons, $p_{\text{T}}^{\ell} > 20\,\text{GeV}/c$	43.3	945	1778	1858
$\not{p}_T > 30\,\text{GeV}$	32.7	80	1252	1600
2 jets, $P_{\text{T}}^{\text{jet}} > 50\,\text{GeV}/c$	19.8	31	225	596
$m_Z \pm 6\,\text{GeV}$	16.8	24	180	29
one b-tag	8.2	10	28	10
$m_t \pm 24\,\text{GeV}$	6.1	0	2	5

Table 3. Selection cuts applied to the likelihood-based analyses

Selection level	$t \to Zq$	$t \to \gamma q$	$t \to gq$ "3 jets"	$t \to gq$ "4 jets"
General selection			1 lepton, 2 jets, $\not{p}_{\text{T}} > 20\,\text{GeV}/c$	
Preselection	3 leptons, 2 jets	1 photon	3 jets, 1 b-tag	4 jets, 1 b-tag
Final selection	$p_{\text{T}j1} > 30\,\text{GeV}/c$, 1 b-tag, 2 ℓ same flavour, oppos. charge	$p_{\text{T}\gamma} > 75\,\text{GeV}/c$, 1 b-tag	$E_{\text{vis}} > 300\,\text{GeV}$, $p_{\text{T}g} > 75\,\text{GeV}/c$, $m_{qg} > 125\,\text{GeV}/c$, $m_{qg} < 200\,\text{GeV}/c$	$E_{\text{vis}} > 300\,\text{GeV}$, $p_{\text{T}g} > 100\,\text{GeV}/c$, $m_{qg} > 150\,\text{GeV}/c$, $m_{qg} < 190\,\text{GeV}/c$

Table 4. The number of selected background events, normalised to $L = 10\,\text{fb}^{-1}$, and signal efficiencies in the $t \to Zq$ channel for the preselection and final selection levels, obtained with a likelihood-based analysis, are shown

Description of cuts	Signal $t \to Zq$ ε (%)	Background processes Z+jets Nevt	$Z+W$ Nevt	$t\bar{t}$ Nevt	single t Nevt
Preselection	17.0	78.7	29.8	1514.2	24.3
Final Selection	7.1	13.1	1.7	434.2	4.8

is $\sigma(m_{\ell\ell j}) = 14\,\text{GeV}/c^2$. Accepted combinations were required to lie within $\pm 24\,\text{GeV}/c^2$ ($\sim 2\sigma$) around the known top quark mass. This top mass window removes almost completely the remaining background and the final signal efficiency is 6.1% with a total background of 7 events for an integrated luminosity of $100\,\text{fb}^{-1}$.

Table 2 summarises the effects of the sequential application of the above described various analysis cuts on the background samples and on the sample of 20 565 signal events of the topology $t\bar{t} \to ZqWb \to \ell^+\ell^- j\ell\nu b$.

3.1.3 Likelihood-based analysis: leptonic mode

The leptonic decay mode was also studied with a likelihood-based analysis. A general selection criteria was defined for the likelihood-based analyses: events were required to have at least one isolated lepton with $p_{\text{T}} > 25\,\text{GeV}/c$ and at least two jets with $p_{\text{T}} > 20\,\text{GeV}/c$ in the final state. Both the lepton and the jets were required to have $|\eta| < 2.5$. Additionally, the transverse missing momentum had to be greater than $20\,\text{GeV}/c$. Table 3 summarises the cuts performed in the likelihood-based analysis.

At the preselection, events were accepted if they had at least two additional isolated leptons (apart from the one already required by the general selection criteria) with $p_{\text{T}} > 10\,\text{GeV}/c$ and $|\eta| < 2.5$. For the likelihood-based analyses, all the background samples were normalised to $L = 10\,\text{fb}^{-1}$. The number of selected background events and the signal efficiency are shown in Table 4. The dis-

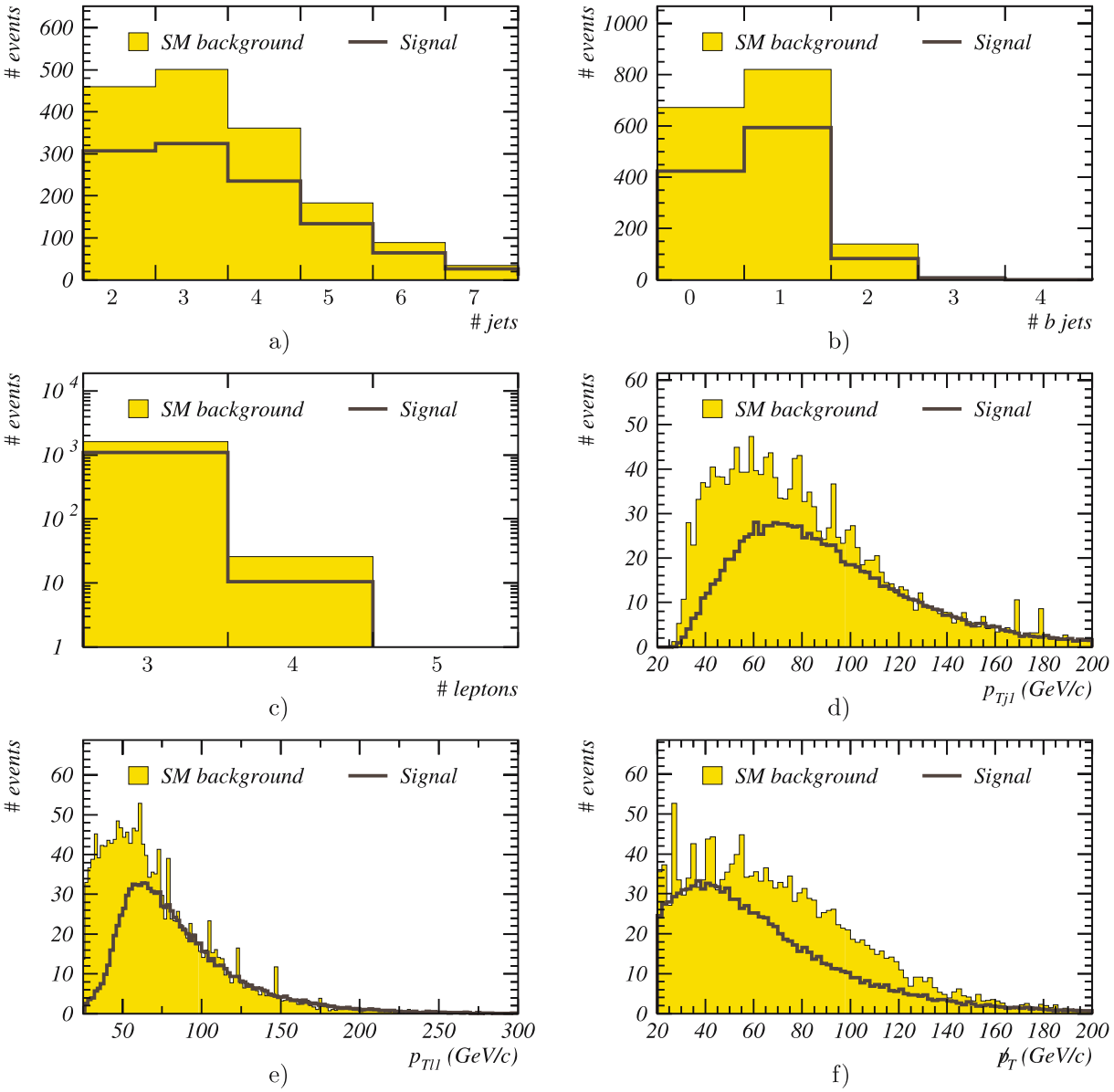

Fig. 5. The distributions of relevant variables for the $t \to Zq$ channel are shown after the preselection level: **a** number of jets; **b** number of b-jets; **c** number of leptons; **d** transverse momentum of the first jet; **e** transverse momentum of the first lepton and **f** missing transverse momentum. The SM background is normalised to $L = 10\,\text{fb}^{-1}$ and the signal has an arbitrary normalization, but the same in all plots of this figure

tribution of relevant variables at this level are shown in Fig. 5.

The final event selection was done by requiring the leading jet to have $p_{\text{T}} > 30\,\text{GeV}/c$. One of the jets had to be tagged as a b-jet. Additionally, in order to be compatible with the $Z \to \ell^+\ell^-$ decay, two of the three leptons present in the final state were required to have opposite charges and the same flavour (electron or muon). The number of selected SM events and the signal efficiency at the final selection level are shown in Table 4. The dominant contribution for the single top background is the t-channel. No QCD ($b\bar{b}$) and W+jets events passed the final selection criteria, within the generated statistics (3.75×10^8 and 3.5×10^7 events, respectively).

The reconstruction of the Z mass was done by calculating the $\ell^+\ell^-$ invariant mass[2] ($m_{\ell^+\ell^-}$) and is shown in Fig. 6a. The reconstruction of the mass of the t-quark which decayed through FCNC ($m_{j\ell^+\ell^-}$) was done by associating the non-b jet with the $\ell^+\ell^-$ pair. If more than one non-b jet was present, the one with highest p_{T} was chosen. The signal and SM distributions of $m_{j\ell^+\ell^-}$ are shown in Fig. 6b. The decay of the other t-quark ($t \to b\ell\nu$) cannot be directly reconstructed due to the presence of an undetected neutrino in the final state. Nevertheless, the

[2] In the case where more than one pair of leptons had the same flavour and opposite charges, the pair with highest p_{T} was chosen.

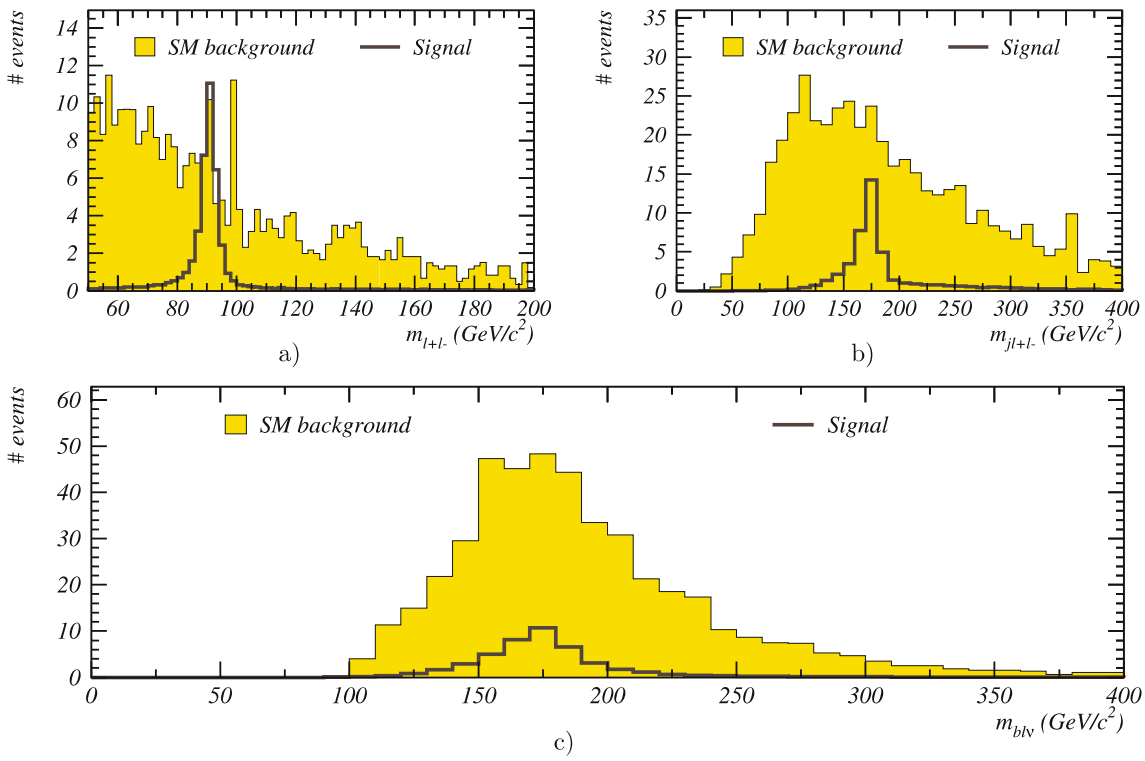

Fig. 6. The reconstructed masses after the final selection level for the $t \to Zq$ channel are shown: **a** Z boson ($\ell^+\ell^-$ invariant mass); **b** t-quark with FCNC decay ($j\ell^+\ell^-$ invariant mass) and **c** t-quark with SM decay ($b\ell\nu$ invariant mass). The SM background is normalised to $L = 10\,\text{fb}^{-1}$ and the signal has an arbitrary normalization, but the same in all plots of this figure

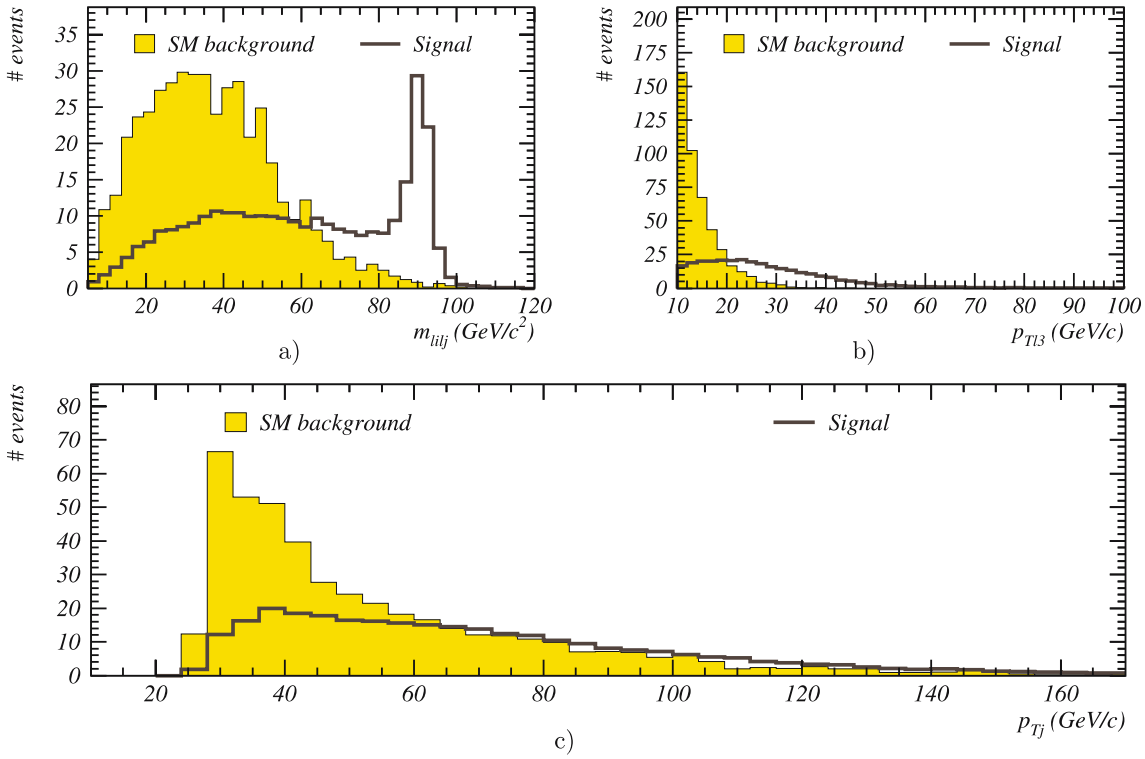

Fig. 7. The distribution of the variables based on which the p.d.f. were built are shown ($t \to Zq$ channel): **a** two leptons minimum mass (only the first three leptons were considered); **b** transverse momentum of the third lepton and **c** transverse momentum of the most energetic non b-jet. The $j\ell^+\ell^-$ invariant mass was also used as p.d.f. and is shown in Fig. 6b. The SM background is normalised to $L = 10\,\text{fb}^{-1}$ and the signal has an arbitrary normalization, but the same in all plots of this figure

neutrino four-momentum can be estimated by assuming the transverse missing energy to be the transverse neutrino momentum. The longitudinal component can be determined, with a quadratic ambiguity, by constraining the W mass (calculated as the invariant mass of the neutrino and the most energetic remaining lepton) to its known central value ($m_W = 80.4\,\mathrm{GeV}/c^2$ [31]). The mass of t-quark with a SM decay, shown in Fig. 6c, was reconstructed by associating the b-jet with the reconstructed W. The quadratic ambiguity was removed by choosing the solution closer to $m_t = 175\,\mathrm{GeV}/c^2$.

Following the final selection, a likelihood-based type of analysis was applied. Signal ($\mathcal{P}_i^{\mathrm{signal}}$) and background-like ($\mathcal{P}_i^{\mathrm{back}}$) probabilities were computed using probability density functions (p.d.f.), constructed from relevant physical variables. The signal $\mathcal{L}_{\mathrm{S}} = \prod_{i=1}^{n} \mathcal{P}_i^{\mathrm{signal}}$ and background $\mathcal{L}_{\mathrm{B}} = \prod_{i=1}^{n} \mathcal{P}_i^{\mathrm{back}}$ likelihoods (n is the number of p.d.f.) were used to built the discriminant variable, defined as $L_R = \ln(\mathcal{L}_{\mathrm{S}}/\mathcal{L}_{\mathrm{B}})$, assuming uncorrelated variables.

For the $t \to Zq$ channel the p.d.f. were based on the following physical distributions (c.f. Fig. 7):

- minimum invariant mass ($m_{\ell_i \ell_j}$) of the three possible combinations of two leptons (only the three leading leptons were considered);
- transverse momentum of the third lepton ($p_{\mathrm{T}l3}$);
- the $j\ell^+\ell^-$ invariant mass and
- the transverse momentum of the most energetic non-b jet ($p_{\mathrm{T}j}$).

The L_R distributions for SM background and signal are shown, after the final selection, in Fig. 8. The number of expected SM background as a function of the signal efficiency obtained by cutting the discriminant variable is shown in Fig. 9.

3.2 $t \to \gamma q$ channel

The $t\bar{t}$ final states corresponding to the FCNC decay $t \to \gamma q$ are characterised by the presence of a high p_{T} photon and a light jet from the top quark decay. Since the existence of the photon is not sufficient to reduce the QCD background, only the leptonic decays of the W (originated from the SM decay of the other top quark) were considered. The final states corresponding to these signal events are characterised by a topology with two jets (one b-jet from the SM top decay), one high p_{T} photon, one lepton and missing transverse momentum from the undetected neutrino. Following a previous analysis [25], a new one was developed [24] and is described below.

After applying the general selection criteria described in Sect. 3.1.3, a preselection was defined by requiring the

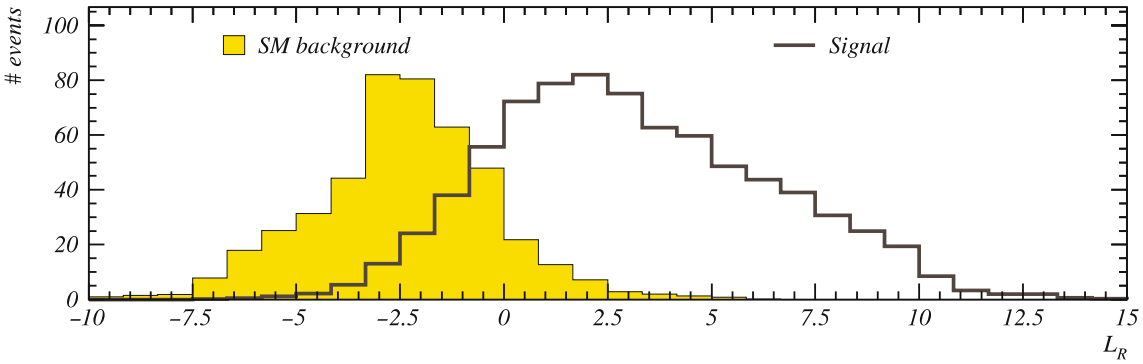

Fig. 8. SM background and signal discriminant variable distributions for the $t \to Zq$ channel are shown. The SM background is normalised to $L = 10\,\mathrm{fb}^{-1}$ and the signal has an arbitrary normalization

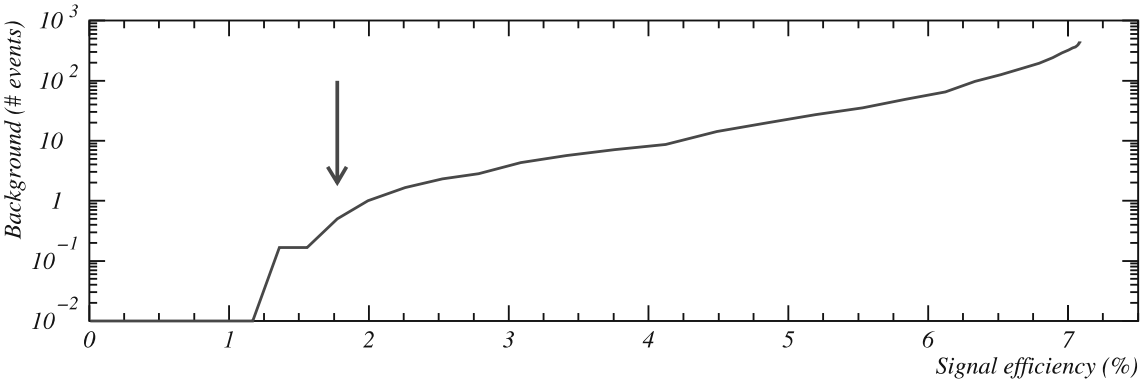

Fig. 9. The number of expected SM background as a function of the signal efficiency for the $t \to Zq$ channel is shown. The SM background is normalised to $L = 10\,\mathrm{fb}^{-1}$. The arrow shows the point with best $S/\sqrt{B}$

events to have at least one photon with $p_{\mathrm{T}} > 50\,\mathrm{GeV}/c$ and $|\eta| < 2.5$. Additionally, in order to prevent events to be simultaneously assigned to the $t \to Zq$ and $t \to \gamma q$ channels, a maximum of two leptons in the final state were allowed. The number of selected SM background events and the signal efficiency at the preselection level are shown in Table 5. The distributions of relevant variables for SM background and signal are shown in Fig. 10.

The final event selection was done by requiring the leading photon to have $p_{\mathrm{T}} > 75\,\mathrm{GeV}/c$ and one of the two jets with highest p_{T} to be tagged as a b-jet (only one b-jet was allowed). This selection largely reduces the background, being $t\bar{t}_{\mathrm{SM}}$ the dominant contribution, as can be seen in Table 5. The FCNC top decay was reconstructed using the non-b jet and the photon (in the cases were more than one photon or non-b quark were available, the one with higher p_{T} was chosen). No QCD ($b\bar{b}$) and W+jets events, within the generated statistics, passed the final selection criteria. Just like for the $t \to Zq$ channel, a likelihood-based type of analysis was used. The p.d.f. were built based on the following variables (c.f. Fig. 11):

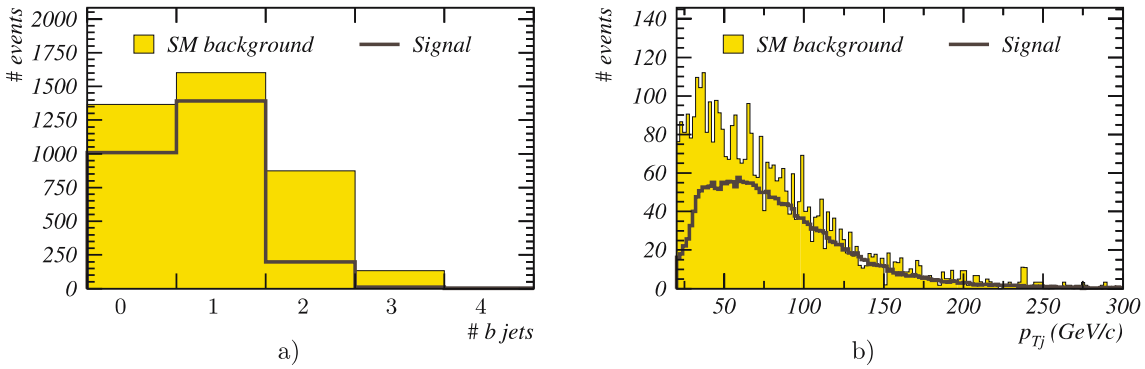

Fig. 10. The distributions of relevant variables for the $t \to \gamma q$ channel are shown after the preselection level: **a** number of b-jets and **b** transverse momentum of the $c(u)$-jet. The SM background is normalised to $L = 10\,\mathrm{fb}^{-1}$ and the signal has an arbitrary normalization, but the same in all plots of this figure

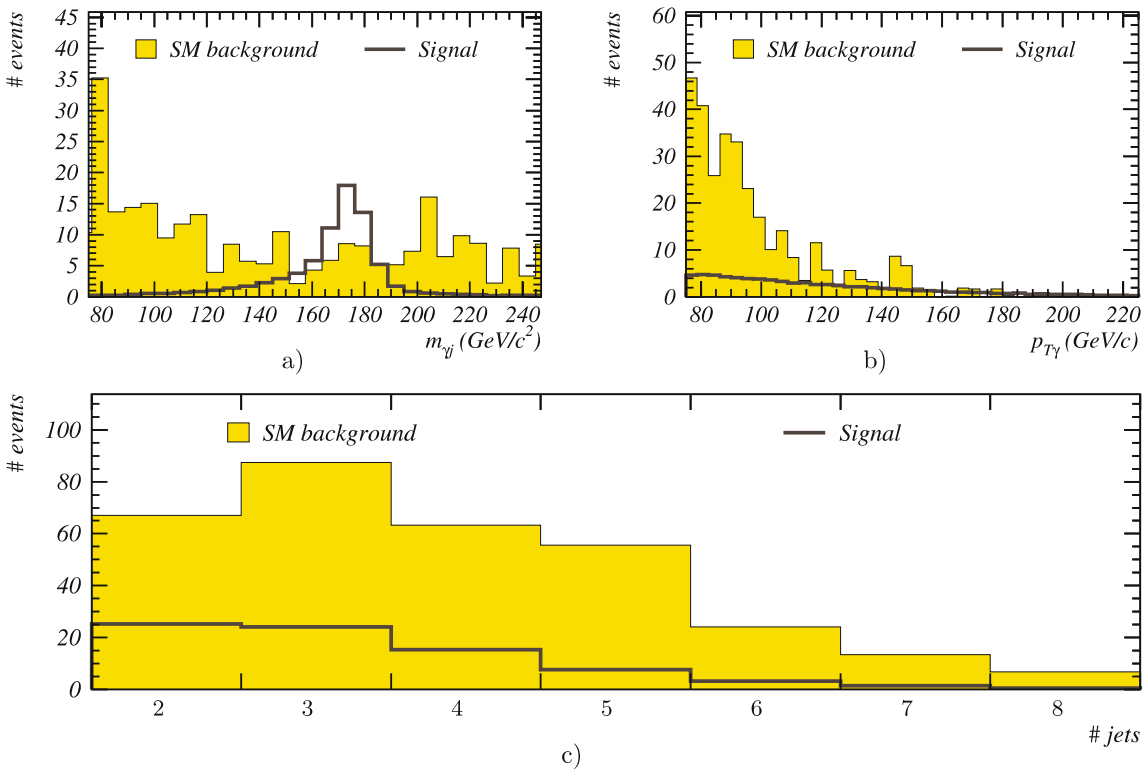

Fig. 11. The distribution of the variables based on which the p.d.f. were built are shown ($t \to \gamma q$ channel): **a** reconstructed mass of the t-quark with FCNC decay ($j\gamma$ invariant mass); **b** transverse momentum of the photon and **c** number of jets. The SM background is normalised to $L = 10\,\mathrm{fb}^{-1}$ and the signal has an arbitrary normalization, but the same in all plots of this figure

Table 5. The number of selected background events, normalised to $L = 10\,\text{fb}^{-1}$, and signal efficiencies in the $t \to \gamma q$ channel for the preselection and final selection levels, obtained with a likelihood-based analysis, are shown

Description of cuts	Signal $t \to \gamma q$ ε (%)	Background processes Z+jets Nevt	$Z+W$ Nevt	$t\bar{t}$ Nevt	single t Nevt
Preselection	23.3	584.2	325.7	2832.4	206.2
Final Selection	6.9	15.2	7.7	271.6	23.0

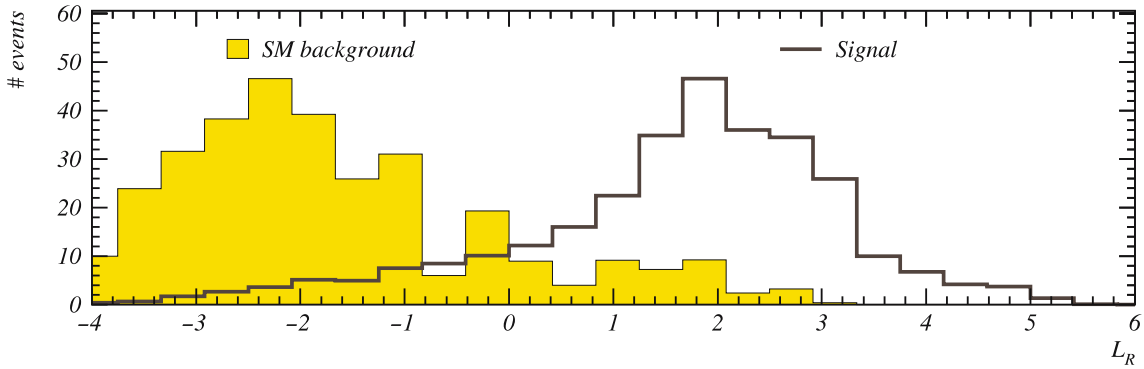

Fig. 12. SM background and signal discriminant variable distributions for the $t \to \gamma q$ channel are shown. The SM background is normalised to $L = 10\,\text{fb}^{-1}$ and the signal has an arbitrary normalization

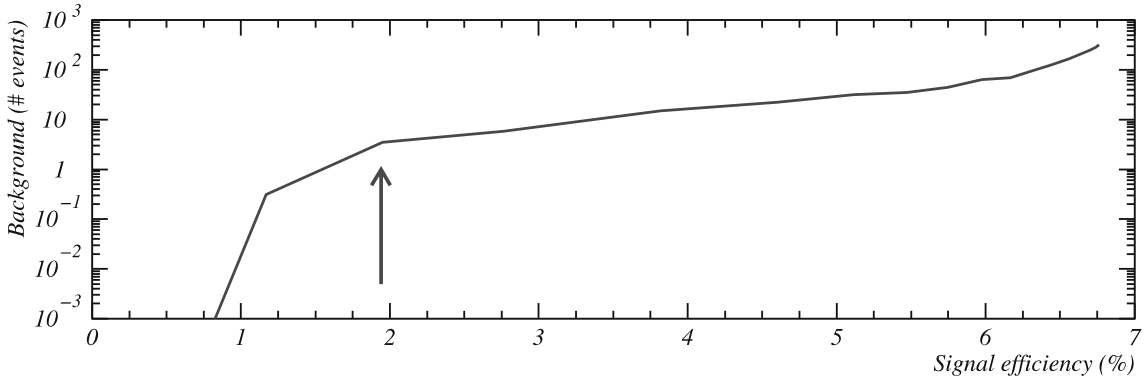

Fig. 13. The number of expected SM background as a function of the signal efficiency for the $t \to \gamma q$ channel is shown. The SM background is normalised to $L = 10\,\text{fb}^{-1}$. The *arrow* shows the point with best $S/\sqrt{B}$

– the mass of the t-quark with FCNC decay, reconstructed from the photon and the non-b jet ($m_{j\gamma}$);
– the transverse momentum of the leading photon ($p_{\text{T}\gamma}$) and
– the number of jets.

The discriminant variables distributions for signal and SM expectation are shown in Fig. 12 and the number of expected SM background as a function of the signal efficiency obtained by cutting the discriminant variable is shown in Fig. 13.

3.3 $t \to gq$ channel

The final states of $t\bar{t}$ events with one of the top quarks decaying into a gluon, $t \to gq$, are characterised by the presence of a high p_{T} gluon and a light jet from the top quark decay. Only the leptonic decays of the W (originated from the SM decay of the other top quark) were taken into account, otherwise the final state would be fully hadronic and the signal would be overwhelmed by the QCD background. The final states are thus characterised by the existence of at least three jets (one b-jet from the SM top decay), one lepton and missing transverse momentum from the undetected neutrino.

Although no previous analyses have been performed for the $t \to gq$ decay, the anomalous coupling tgq in top production was studied in the past [22, 26]. A new analysis dedicated to the $t \to gq$ decay was developed [24] and is described here.

As in this topology the FCNC top decay corresponds to a fully hadronic final state, a more restrictive event selection was necessary. The general selection criteria of

Sect. 3.1.3 was applied to the events. At the preselection, events were required to have only one lepton and no photons with transverse momentum above $p_{\mathrm{T}} > 5\,\mathrm{GeV}/c$, to reject events assigned to the other FCNC channels. The total visible energy (E_{vis}) had to be greater than 300 GeV. At least three jets with $|\eta| < 2.5$ and $p_{\mathrm{T}} > 20\,\mathrm{GeV}/c$ were required. For the leading jet the cut was increased to $40\,\mathrm{GeV}/c$. The events were then classified as "3 jets" or "4 jets" if they had exactly three jets or at least 4 jets, respectively.

3.3.1 The "3 jets" sample

The preselection was completed by requiring only one b-tagged jet in the event. The gluon jet was assumed to be the non-b jet with the highest transverse momentum. This distribution is shown in Fig. 14, together with the mass of the t-quark with FCNC decay (m_{qg}), reconstructed from the non-b jets. The mass of the t-quark with SM decay ($m_{b\ell\nu}$, reconstructed according to Sect. 3.1.3) is also shown. The number of selected SM background events and the signal efficiency at this level are presented in Table 6. The final event selection was done by requiring the gluon to have $p_{\mathrm{T}} > 75\,\mathrm{GeV}/c$ and $125 < m_{qg} < 200\,\mathrm{GeV}/c^2$. No generated QCD ($b\bar{b}$) events passed the final selection criteria.

As for the other channels, a likelihood-based type of analysis was adopted, using the following variables to build the p.d.f. (c.f. Fig. 15):

- the qg invariant mass,
- the $b\ell\nu$ invariant mass,
- transverse momentum of the b-jet ($p_{\mathrm{T}\,b}$),
- transverse momentum of the second non-b jet ($p_{\mathrm{T}\,j}$) and
- angle between the lepton and the gluon ($\alpha_{\ell g}$).

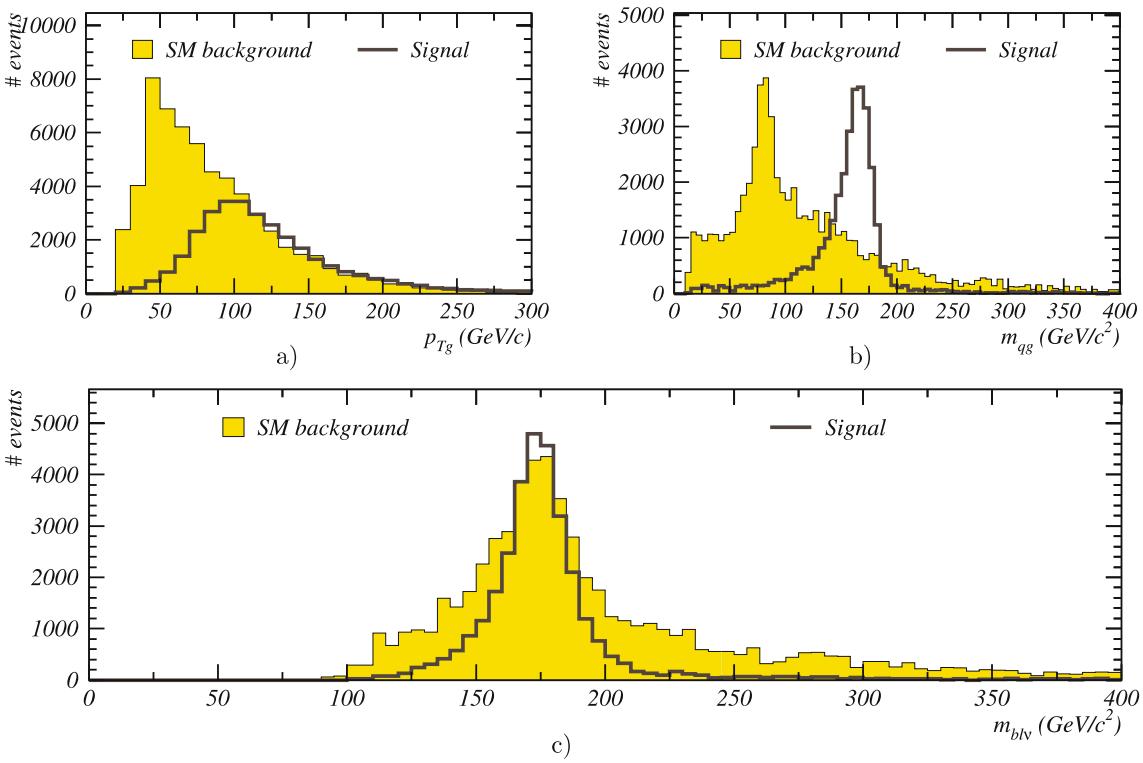

Fig. 14. The distributions of relevant variables for the $t \to gq$ ("3 jets") channel are shown after the preselection level: **a** transverse momentum of the gluon; **b** the qg invariant mass and **c** the $b\ell\nu$ invariant mass. The SM background is normalised to $L = 10\,\mathrm{fb}^{-1}$ and the signal has an arbitrary normalization, but the same in all plots of this figure

Table 6. The number of selected background events, normalised to $L = 10\,\mathrm{fb}^{-1}$, and signal efficiencies in the $t \to gq$ channel ("3 jets") for the preselection and final selection levels, obtained with a likelihood-based analysis, are shown

Description of cuts	Signal $t \to gq$ ε (%)	Background processes Z+jets Nevt	$Z+W$ Nevt	$t\bar{t}$ Nevt	single t Nevt	W+jets Nevt
Preselection	1.6	1356.6	427.1	24 366.7	11 328.2	23 320.3
Final Selection	1.2	157.1	22.1	4985.6	1187.9	1813.3

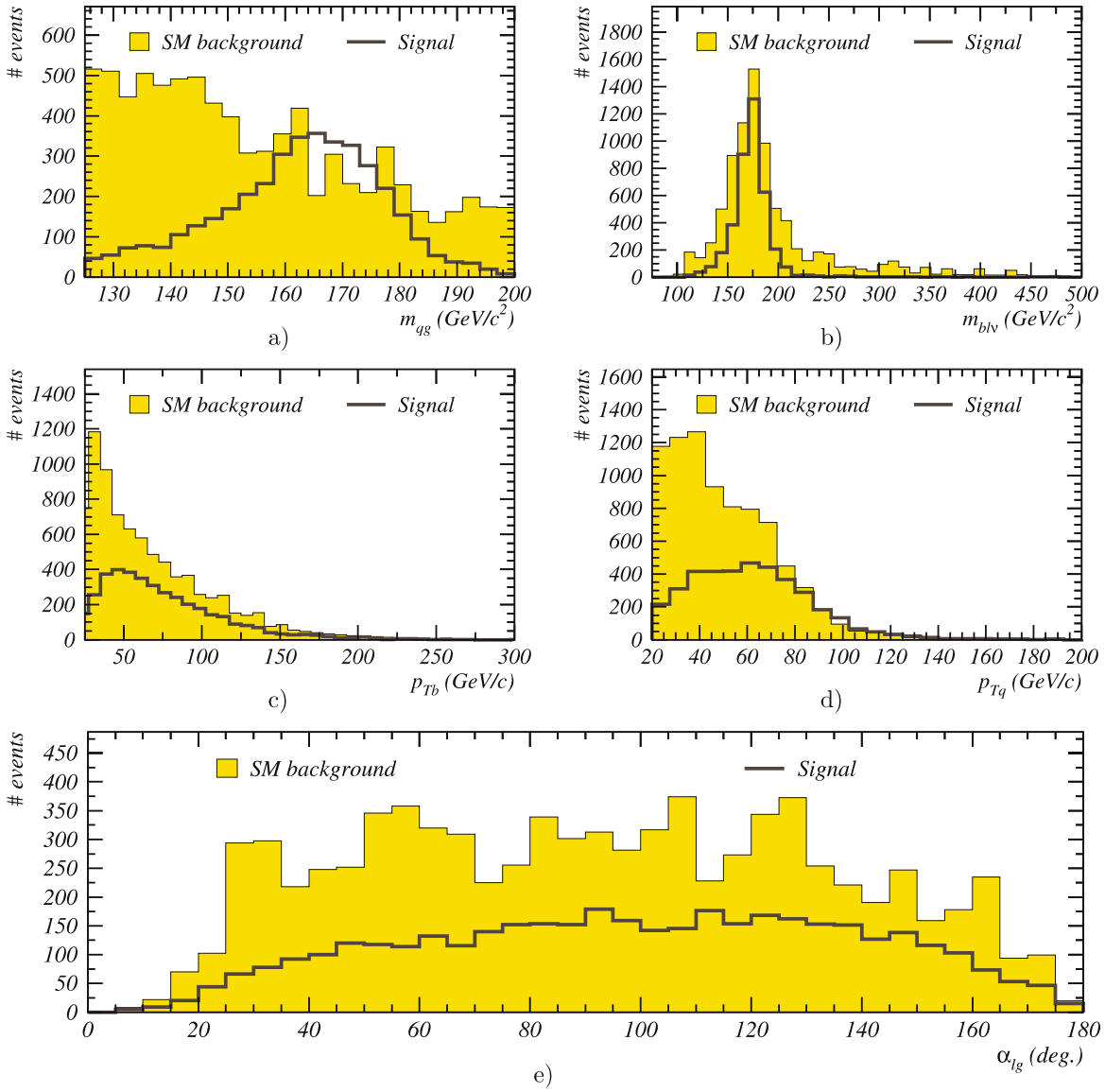

Fig. 15. The distribution of the variables based on which the p.d.f. were built are shown ($t \to gq$ channel – "3 jets") **a** the qg invariant mass; **b** the $b\ell\nu$ invariant mass; **c** transverse momentum of the b-jet; **d** transverse momentum of the $c(u)$-jet and **e** angle between the lepton and the gluon. The SM background is normalised to $L = 10\,\text{fb}^{-1}$ and the signal has an arbitrary normalization, but the same in all plots of this figure

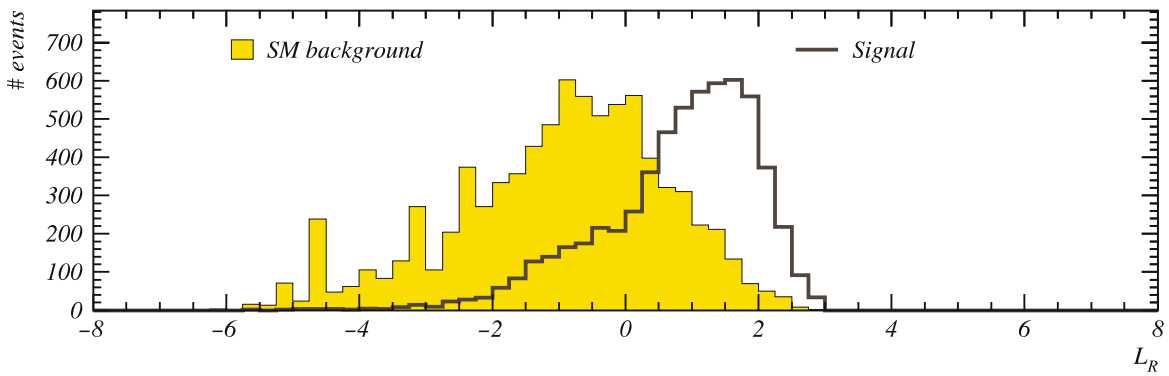

Fig. 16. Expected background and signal discriminant variable distributions for the $t \to gq$ channel with the number of jets equal to three. The SM background is normalised to $L = 10\,\text{fb}^{-1}$ and the signal has an arbitrary normalization

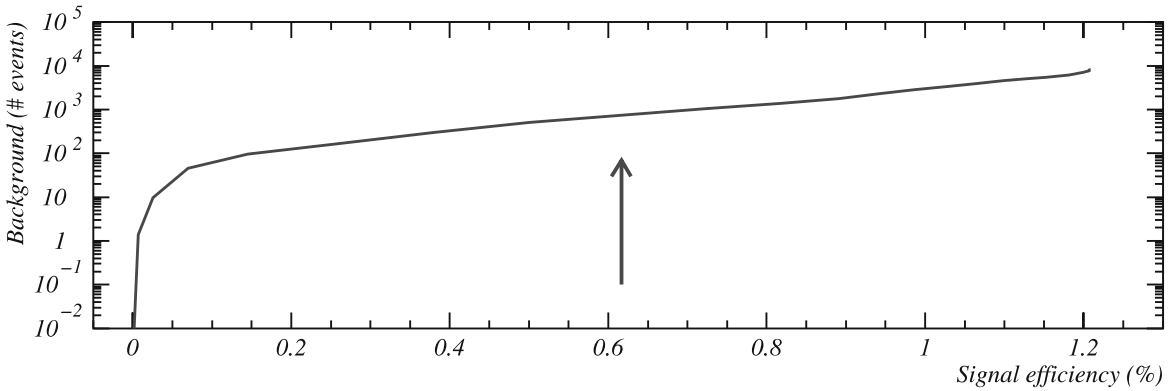

Fig. 17. The number of expected SM background as a function of the signal efficiency for the $t \to gq$ channel with the number of jets equal to three is shown. The SM background is normalised to $L = 10\,\mathrm{fb}^{-1}$. The arrow shows the point with best $S/\sqrt{B}$

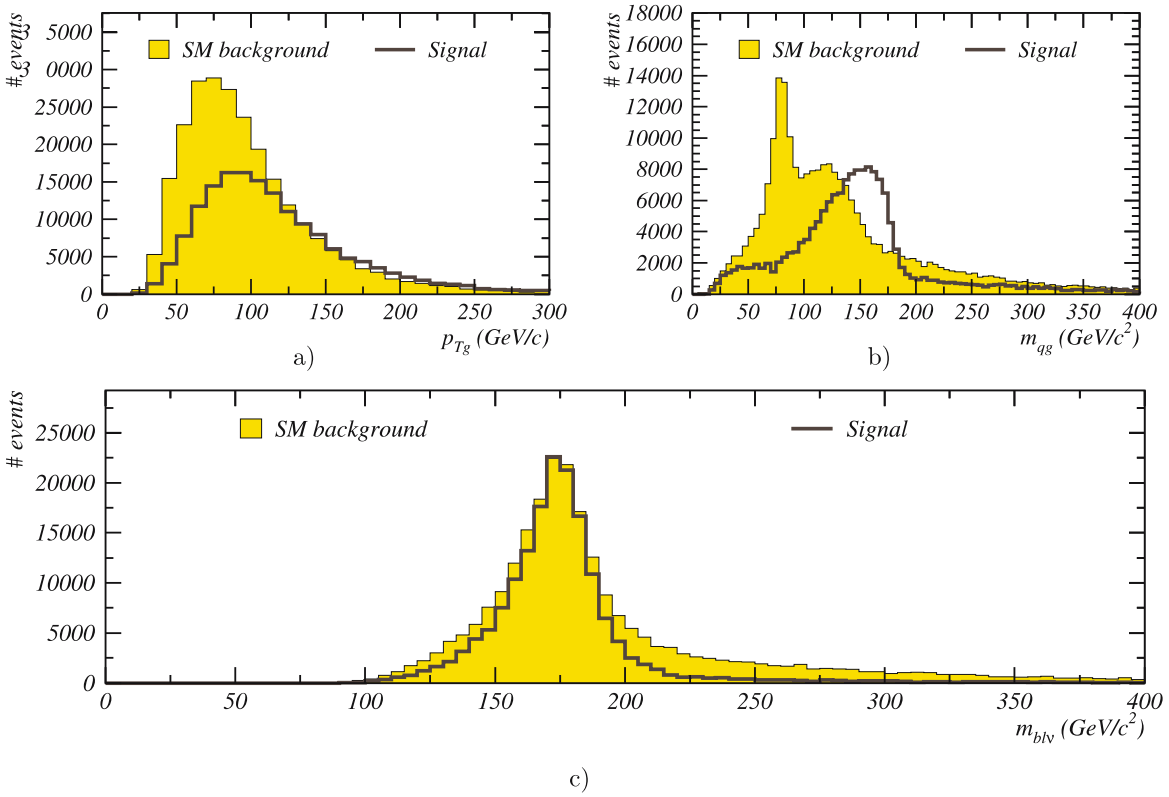

Fig. 18. The distributions of relevant variables for the $t \to gq$ ("4 jets") channel are shown after the preselection level: **a** transverse momentum of the gluon; **b** the qg invariant mass and **c** the $b\ell\nu$ invariant mass. The SM background is normalised to $L = 10\,\mathrm{fb}^{-1}$ and the signal has an arbitrary normalization, but the same in all plots of this figure

Table 7. The number of selected background events, normalised to $L = 10\,\mathrm{fb}^{-1}$, and signal efficiencies in the $t \to gq$ channel ("4 jets") for the preselection and final selection levels, obtained with a likelihood-based analysis, are shown

Description of cuts	Signal $t \to gq$ ε (%)	Background processes Z+jets Nevt	$Z+W$ Nevt	$t\bar{t}$ Nevt	single t Nevt	W+jets Nevt
Preselection	5.7	1171.0	305.2	216 679.9	14 263.1	12 651.2
Final Selection	1.2	64.3	7.1	9142.1	453.3	379.5

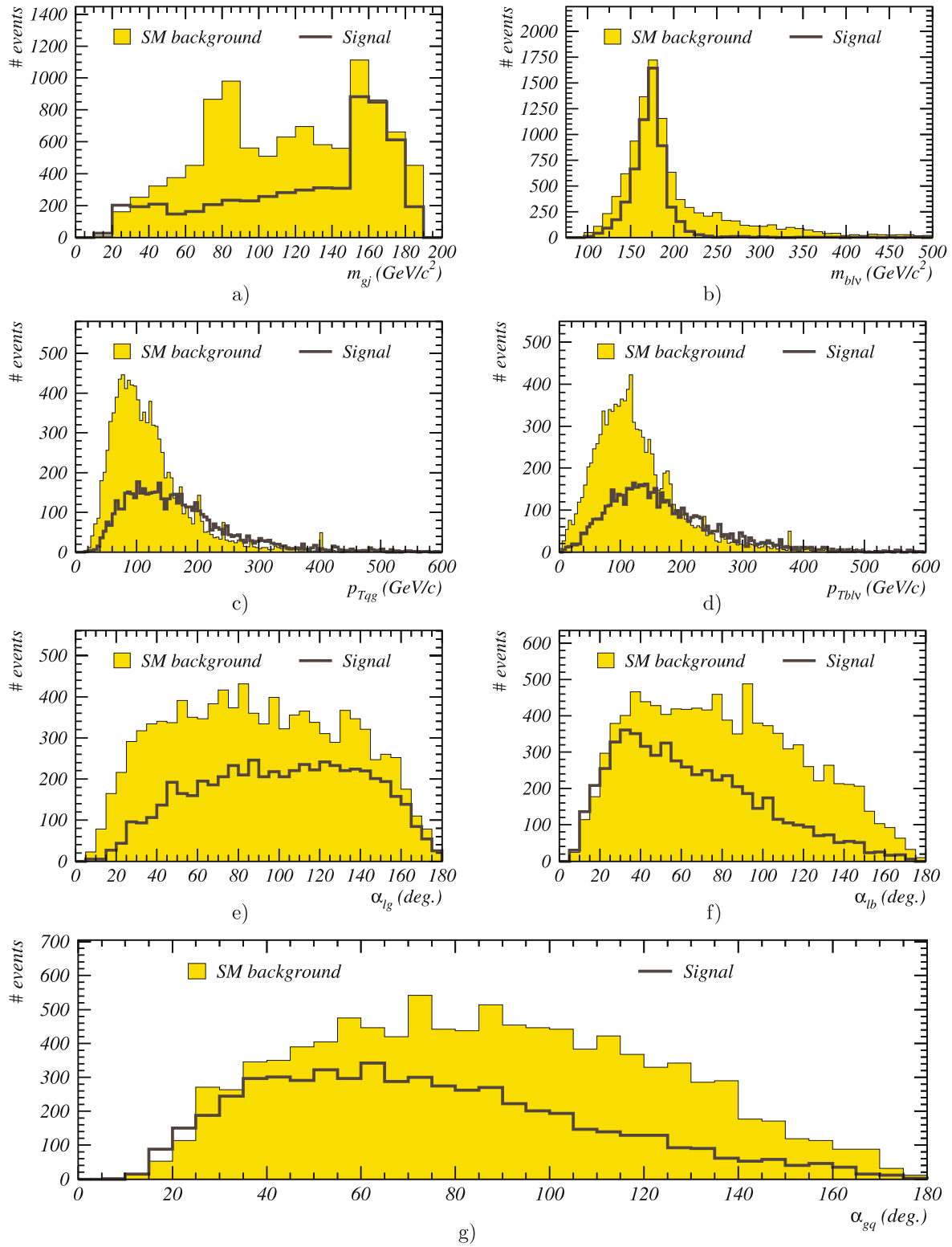

Fig. 19. The distribution of the variables based on which the p.d.f. were built are shown ($t \to gq$ channel – "4 jets") **a** minimum invariant mass of the first and the second non-b jets or the first and the third non-b jets; **b** the $b\ell\nu$ invariant mass; **c** reconstructed transverse momentum of the qg; **d** reconstructed transverse momentum of the $b\ell\nu$; **e** angle between the lepton and the gluon; **f** angle between the lepton and the b-jet and **g** angle between the gluon and the second non-b jet. The SM background is normalised to $L = 10\,\mathrm{fb}^{-1}$ and the signal has an arbitrary normalization, but the same in all plots of this figure

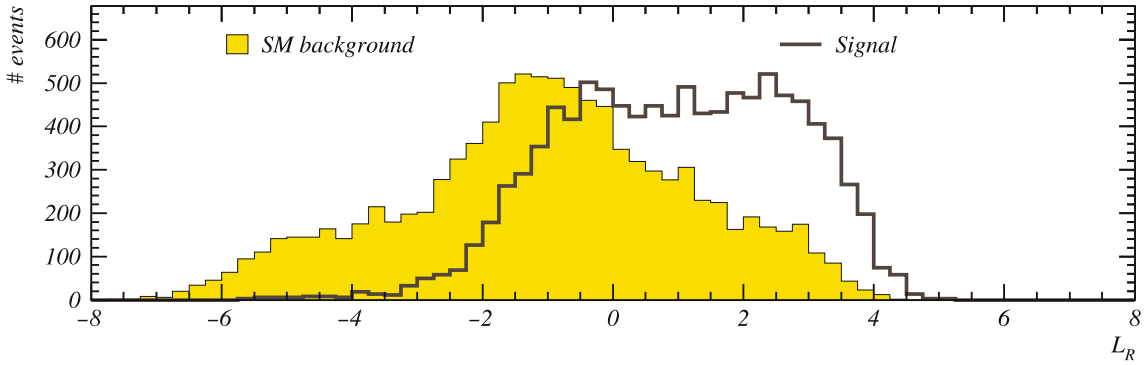

Fig. 20. Expected background and signal discriminant variable distributions for the $t \to gq$ channel with the number of jets greater than three. The SM background is normalised to $L = 10\,\text{fb}^{-1}$ and the signal has an arbitrary normalization

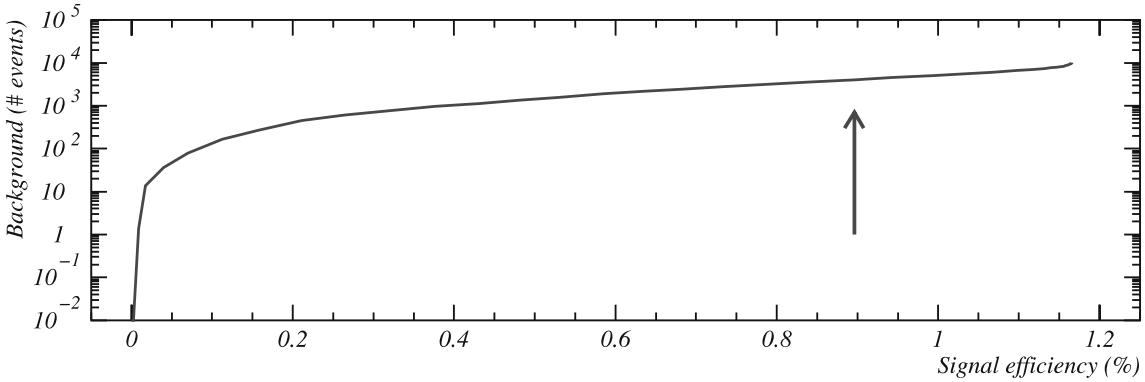

Fig. 21. The number of expected SM background as a function of the signal efficiency for the $t \to gq$ channel with the number of jets greater than three is shown. The SM background is normalised to $L = 10\,\text{fb}^{-1}$. The *arrow* shows the point with best $S/\sqrt{B}$

The signal and background discriminant variable distributions are shown in Fig. 16. The number of expected SM background as a function of the signal efficiency obtained by cutting the discriminant variable is shown in Fig. 17.

3.3.2 The "4 jets" sample

For this topology, the preselection was completed by requiring the fourth jet to have $p_{\text{T}} > 20\,\text{GeV}/c$ and $|\eta| < 2.5$. Only one b-tagged jet, which had to be among the first four, was allowed in the event. The gluon jet was assumed to be the non-b jet with the highest transverse momentum. This distribution is shown in Fig. 18, together with the mass of the t-quark with FCNC decay (m_{gj}), reconstructed from the two non-b jets with the highest transverse momenta. The mass of the t-quark with SM decay is also shown. The number of selected SM background events and the signal efficiency at this level are presented in Table 7.

The final selection was defined by requiring the gluon transverse momentum to be above $100\,\text{GeV}/c$ and the reconstructed mass of the t-quark with FCNC decay above $150\,\text{GeV}/c^2$ and below $190\,\text{GeV}/c^2$. As for the "3 jets" channel, no generated QCD ($b\bar{b}$) passed the final selection criteria.

After the final selection, the p.d.f. were built based on the following physical distributions (c.f. Fig. 19):

– minimum invariant mass of the leading and the second non-b jets or the leading and the third non-b jets (m_{gj}),
– the $b\ell\nu$ invariant mass,
– transverse momentum of qg,
– transverse momentum of $b\ell\nu$,
– angle between the lepton and the gluon ($\alpha_{\ell g}$),
– angle between the lepton and the b-jet ($\alpha_{\ell b}$) and
– angle between the gluon and the second non-b jet (α_{gq}).

The discriminant variable distributions for signal and SM expectation are shown in Fig. 20, while the number of expected SM background as a function of the signal efficiency obtained by cutting the discriminant variable is shown in Fig. 21.

4 Results and systematic studies

Expected top quark FCNC decay branching ratios sensitivities of the ATLAS experiment were estimated for both the cut-based and likelihood-based analysis under two different hypothesis, as explained in the next subsections.

4.1 Branching ratio sensitivity (5σ significance discovery hypothesis)

Assuming a signal discovery with a 5σ significance, the branching ratio (BR) sensitivity for each channel studied is

estimated by:

$$\mathrm{BR} = \frac{5\sqrt{B\varepsilon_\ell}}{2L\sigma(t\bar{t}_{\mathrm{SM}})\varepsilon_t\varepsilon_\ell}\,, \qquad (5)$$

where $\sigma(t\bar{t}_{\mathrm{SM}}) = 833\,\mathrm{pb}$ [18, 19] is the NLO calculation of the SM cross-section for $t\bar{t}$ production in pp collisions at $\sqrt{s} = 14\,\mathrm{TeV}$. B is the total number of selected background events, ε_t is the signal efficiency convoluted with the appropriate branching ratios and $\varepsilon_\ell = 0.9^n$ is the charged leptons identification efficiency (n is the number of leptons required for each channel). The factor 2 in the denominator takes into account the t and $\bar{t}$ contributions to the BR.

To evaluate the expected branching ratio sensitivities for a 5σ signal significance of discovery in the cut-based analyses, the kinematic cuts were applied in sequence for the signal and backgrounds. In the channels studied using likelihood-based analyses, the expected branching ratio sensitivities were evaluated after applying cuts to the discriminant variables, as given in Table 8 (see also Figs. 9, 13, 17 and 21). These cuts were optimised according to the best $S/\sqrt{B}$ (S is the number of selected signal events). The expected branching ratio sensitivities for a 5σ discovery are shown in Table 9.

4.2 95% confidence level limits (hypothesis of absence of signal)

In the absence of a FCNC top decay signal, expected limits at 95% CL can be derived. These limits were obtained for both the cut-based and the likelihood-based analyses, setting the charged lepton identification efficiency to 90%.

For the cut-based analyses of the $t \to Zq$ channel, the 95% CL upper limits were evaluated considering an integrated luminosity of $100\,\mathrm{fb}^{-1}$. Assuming the Poisson processes with backgrounds, 95% CL upper limits on the number of signal events for both decay modes were derived. The modified frequentist likelihood method [32, 33] was used to evaluate the 95% CL upper limits for the likelihood-based analyses. The full information of the discriminant variables were used to derive 95% CL upper limits on the number of signal events for each channel. No cuts on the discriminant variables were used. Using the NLO calculation for $\sigma(t\bar{t}_{\mathrm{SM}})$, these limits were then converted into limits on the branching ratio for each of the studied FCNC top decay channels. The expected 95% confidence level limits on the branching ratios are summarised in Table 10.

Table 8. The number of selected background events (normalised to $L = 10\,\mathrm{fb}^{-1}$) and signal efficiencies (convoluted with the appropriate branching ratios) for each channel of the likelihood-based analyses after the specified L_R cut are shown

channel		L_R cut	B	ε_t (%)
$t \to Zq$		> 5.62	0.50	0.06
$t \to \gamma q$		> 2.71	3.48	0.62
$t \to gq$	"3 jets"	> 1.13	734.1	0.20
	"4 jets"	> -0.38	4033.9	0.29

4.3 Systematic uncertainties and analyses stability

The effect of different systematic sources of uncertainty on the limits evaluation was studied for both the cut-based and the likelihood-based analyses. This estimation was done by considering the changes on the central values of the signal efficiency, number of background events and likelihood ratio distributions.

For the cut-based analysis of the $t \to Zq$ channel several systematic uncertainties were studied. The effect of the mass window cut applied to the top quark (which decayed through the FCNC channel) was studied by selecting events in a more restrictive window i.e., $m_t \pm 12\,\mathrm{GeV}/c^2$ ($\sim\sigma$). This results in a increase 12% (8%) on the 95% CL limit for the hadronic (leptonic) mode. Varying the p_{T} cut applied to the jets from 50 to $40\,\mathrm{GeV}/c^2$ (leptonic mode) results in a relative change of the limit of 23% [34]. This variation significantly increases the $t\bar{t}$, the WZ and partly the $Z+$jets backgrounds. Changing the lepton isolation criteria (to $\Delta R = 0.2$) gives a relative change of 1% in the 95% CL limit.

For the likelihood-based analysis of the leptonic mode of $t \to Zq$, the $t \to \gamma q$ and the $t \to gq$ channels, the following systematic uncertainties were considered. The ef-

Table 9. The branching ratio sensitivity for each channel in the 5σ discovery hypothesis is shown. The results for a luminosity of $L = 10$ and $100\,\mathrm{fb}^{-1}$ are presented. The values shown for the likelihood-based analyses were obtained after applying the cuts described in Table 8. The values presented for the cut-based analyses of the $t \to Zq$ channel, with $L = 10\,\mathrm{fb}^{-1}$, and of the $t \to \gamma q$ channel were taken from [25]

channel	type		BR ($L = 10\,\mathrm{fb}^{-1}$)	BR ($L = 100\,\mathrm{fb}^{-1}$)
$t \to Zq$	cut-based	hadronic	1.7×10^{-3} [25]	5.0×10^{-4}
		leptonic	4.7×10^{-4} [25]	1.1×10^{-4}
	likelihood-based	leptonic	4.4×10^{-4}	1.4×10^{-4}
$t \to \gamma q$	cut-based		–	1.0×10^{-4} [25]
	likelihood-based		9.4×10^{-5}	3.0×10^{-5}
$t \to gq$	likelihood-based	"3 jets"	4.3×10^{-3}	1.4×10^{-3}
		"4 jets"	6.9×10^{-3}	2.2×10^{-3}

Table 10. The expected 95% confidence level limits on the FCNC top decays branching ratio in the absence of signal hypothesis are shown. The results for a luminosity of $L = 10$ and $100\,\mathrm{fb}^{-1}$ are presented

channel	type		BR ($L = 10\,\mathrm{fb}^{-1}$)	BR ($L = 100\,\mathrm{fb}^{-1}$)
$t \to Zq$	cut-based	hadronic	–	2.7×10^{-4}
		leptonic	–	6.3×10^{-5}
		combined	–	5.5×10^{-5}
	likelihood-based	leptonic	3.1×10^{-4}	6.1×10^{-5}
$t \to \gamma q$	likelihood-based		4.1×10^{-5}	1.2×10^{-5}
$t \to gq$	likelihood-based	"3 jets"	1.6×10^{-3}	4.8×10^{-4}
		"4 jets"	2.4×10^{-3}	7.5×10^{-4}
		combined	1.3×10^{-3}	4.2×10^{-4}

Table 11. Absolute value of the maximum relative changes on the 95% confidence level expected limits for each FCNC top decay branching ratio evaluated with the likelihood-based analyses. The reference values were presented in Table 10 ($L = 10\,\mathrm{fb}^{-1}$)

Source	$t \to Zq$	$t \to \gamma q$	$t \to gq$	
			(3 jets)	(4 jets)
top mass	18%	13%	8%	7%
$\sigma(t\bar{t})$	11%	11%	9%	7%
PDFs choice	15%	7%	3%	6%
b-tag algorithm efficiency	16%	5%	18%	17%
jet energy calibration	2%	1%	2%	3%
analysis stability	9%	12%	3%	13%
p.d.f.s choice	10%	15%	1%	2%

fect of the top mass uncertainty was evaluated using different Monte Carlo samples with $m_t = 170\,\mathrm{GeV}/c^2$ and $m_t = 180\,\mathrm{GeV}/c^2$. This systematic uncertainty affects both the event kinematics (and consequently the discriminant variables shape) and the value of the $t\bar{t}$ cross-section (used in the limits evaluation). The overall theoretical uncertainty on $\sigma(t\bar{t})$ was estimated in reference [12]. The effect of this uncertainty was studied by allowing a change of 12% on the central value of $\sigma(t\bar{t})$, cross-section used both in the $t\bar{t}_{\mathrm{SM}}$ background normalisation and in the BR limits evaluation, assuming a negligible error on the measurement itself. If the error on the cross-section measurement is, for instance, 5%, the ATLAS sensitivity will be degraded but the change will not affect the order of magnitude of the results shown in this paper. For the $t \to Zq$ and the $t \to \gamma q$ channels, a 5% error gives a maximum change on the limit of 5%. For the $t \to gq$ channels, where the expected number of background is more important, the limit can change by a factor 2 to 3 (depending if it is the 3 or 4 jets topology). A precise measurement of the $t\bar{t}$ cross-section is, for this reason, of utmost importance. The CTEQ 5L PDF set was used in the Monte Carlo generation. A different PDF set (CTEQ 4M [27, 28]) was used to estimate the effect of this choice on the event kinematics. As mentioned in Sect. 2, the ATLFASTB package was used to simulate the b-tag algorithm with a b-tag efficiency of 60%. In order to study the impact of the algorithm with a different efficiency, the b-tagging efficiencies of 50% and 70% were also considered. This source of uncertainty affects the signal efficiency, background estimation and discriminant variable shapes. The impact of the knowledge of the absolute jet energy scale was estimated by recalibrating the reconstructed jet energy. A miscalibration of $\pm 1\%$ for light jets and $\pm 3\%$ for b-jets was used. This uncertainty was found to have a negligible effect on the signal efficiency, background estimation and discriminant variable shapes. A jet energy miscalibration of $\pm 5\%$ for all jets was also considered. For the $t \to Zq$, $t \to \gamma q$ and $t \to gq$ ("3 jets") channels the relative changes on the 95% CL expected limits were found to be below 7%. For the most difficult channel ($t \to gq$ – "4 jets") this effect is more important (up to 12%), due to the tighter selection criteria used to reject the large contribution from background. The stability of the cut-based analysis was studied by changing the preselection and final selection (typically a $\pm 10\%$ variation on the cut values was considered). The discriminant variables were computed using the probability density function sets described in Sect. 3. In order to estimate the effect of a different p.d.f. set, the following changes were studied: in the $t \to Zq$ channel, the $\bar{t}$ reconstruction was done by considering the jet closest to the reconstructed Z in the invariant mass evaluation. Similarly, the $\bar{t}$ mass reconstruction in the $t \to \gamma q$ channel was done using the jet closest to the leading γ. Moreover, the t mass was included in the p.d.f. set and the multiplicity of jets with $|\eta| < 2.5$ was chosen as p.d.f. (instead of the jet multiplicity). In the $t \to gq$

channel, ΔR was used instead of the angles, in the p.d.f.s definition.

The absolute value of the maximum relative effect on the 95% confidence level expected limits on each considered source of systematic uncertainty (the reference values are those presented in Table 10) is shown in Table 11 ($L = 10\,\mathrm{fb}^{-1}$). Although differences up to 20% were observed (caused by the uncertainty of the top mass), the order of magnitude of the expected limits on the BR is not affected by any of the systematic uncertainties considered. Moreover, the change on the selection criteria and on the p.d.f. sets do not have a significant impact on the results.

5 Conclusions

The sensitivity of the ATLAS experiment to the FCNC $t \to qX$ $(X = Z, \gamma, g)$ decays of the top quark was estimated. Different types of analysis (cut-based and likelihood-based) were used to obtain the FCNC branching ratio sensitivities (assuming a 5σ signal significance for discovery) or the 95% CL limits on the FCNC branching ratios (in the absence of signal). The leptonic mode of the $t \to Zq$ channel was studied with both type of analysis which give complementary results: the best limit on the BR assuming a signal discovery with a 5σ significance is obtained with the cut-based analysis, while the 95% CL limit obtained with the likelihood-based analysis using the MFL method (which takes into account the shape of the discriminant variables) is better. The impact of systematic errors on the final results was also studied. The expected branching ratio sensitivities obtained by the different analysis and the previous ones [22, 25, 26] have the same order of magnitude, in the range from 10^{-3} to 10^{-5} (for $L = 10\,\mathrm{fb}^{-1}$).

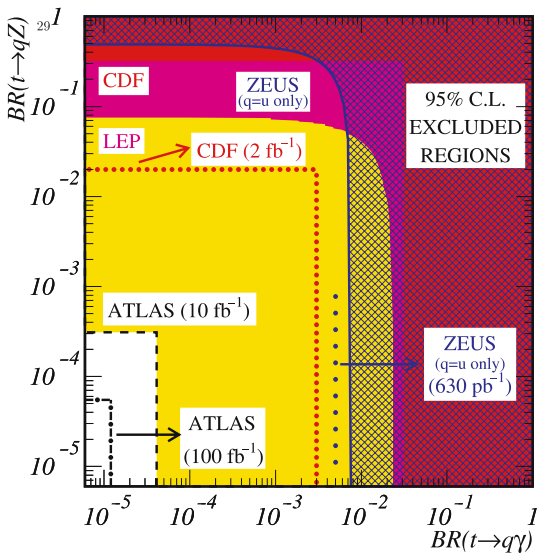

Fig. 22. The present 95% CL limits on the BR($t \to q\gamma$) vs. BR($t \to qZ$) plane are shown. The expected sensitivity at the HERA ($L = 630\,\mathrm{pb}^{-1}$), Tevatron (run II) and LHC is also represented

Even if the SM predicts a much lower branching ratio for the FCNC decays of the top quark, the expected branching ratios obtained in these analysis are several orders of magnitude better then present experimental limits.

The present 95% CL limits and the expected sensitivity at the HERA (ZEUS, $L = 630\,\mathrm{pb}^{-1}$), Tevatron (CDF, run II [35]) and LHC (ATLAS) for BR($t \to q\gamma, qZ$) are summarised in Fig. 22.

Acknowledgements. We thank J.A. Aguilar-Saavedra, M. Cobal, M. David, P. Ferreira, D. Froidevaux, C. Marques, O. Oliveira, E. Richter-Was, R. Santos and S. Slabospitsky for the very useful discussions. This work has been performed within the ATLAS Collaboration, and we thank collaboration members for helpful discussions. We have made use of the physics analysis framework and tools which are the result of collaboration-wide efforts. This work was supported by FCT – Fundação para a Ciência e a Tecnologia through the grants SFRH/BD/13936/2003 and SFRH/BD/18762/2004.

References

1. S.L. Glashow, J. Iliopoulos, L. Maiani, Phys. Rev. D **2**, 1285 (1970)
2. B. Grzadkowski, J.F. Gunion, P. Krawczyk, Phys. Lett. B **268**, 106 (1991)
3. G. Eilam, J.L. Hewett, A. Soni, Phys. Rev. D **44**, 1473 (1991)
4. G. Eilam, J.L. Hewett, A. Soni, Phys. Rev. D **59**, 039 901 (1999)
5. M.E. Luke, M.J. Savage, Phys. Lett. B **307**, 387 (1993)
6. G.M. de Divitiis, R. Petronzio, L. Silvestrini, Nucl. Phys. B **504**, 45 (1997)
7. D. Atwood, L. Reina, A. Soni, Phys. Rev. D **53**, 1199 (1996)
8. F. del Aguila, J.A. Aguilar-Saavedra, R. Miquel, Phys. Rev. Lett. **82**, 1628 (1999)
9. J.A. Aguilar-Saavedra, Acta Phys. Pol. B **35**, 269 (2004) [arXiv:hep-ph/0409342]
10. W. Buchmuller, D. Wyler, Nucl. Phys. B **268**, 621 (1986)
11. W. Hollik, J.I. Illana, S. Rigolin, C. Schappacher, D. Stockinger, Nucl. Phys. B **551**, 3 (1999) [hep-ph/9812298]
12. M. Beneke et al., Top Quark Physics, in: Proceeding of the Workshop on Standard Model Physics (and More) at the LHC, CERN report 2000-004 (2000) 419 [hep-ph/0003033]
13. ALEPH Collaboration, A. Heister et al., Phys. Lett. B **543**, 173 (2002)
14. DELPHI Collaboration, OPAL Collaboration, G. Abbiendi et al., Phys. Lett. B **521**, 181 (2001)
15. L3 Collaboration, P. Achard et al., Phys. Lett. B **549**, 290 (2002)
16. ZEUS Collaboration, S. Chekanov, Phys. Lett. B **559**, 153 (2003)
17. CDF Collaboration, F. Abe et al., Phys. Rev. Lett. **80**, 2525 (1998)
18. R. Bonciani et al., Nucl. Phys. B **529**, 424 (1998)
19. N. Kidonakis, R. Vogt, Phys. Rev. D **68**, 114 014 (2003)
20. J. Campbell et al., Phys. Rev. D **70**, 094 012 (2004)
21. J. Campbell, F. Tramontano, Nucl. Phys. B **726**, 109 (2005)

22. Technical Design Report, ATLAS detector and physics performance, Vol.II, ATL-TDR-15, May 1999
23. L. Chikovani, T. Djobava, ATLAS sensitivity to the Flavour-Changing Neutral Current decay $t \to Zq$, ATL-PHYS-2001-007, March 1999, hep-ex/0205016, May 2002
24. J. Carvalho, N. Castro, A. Onofre, F. Veloso, Study of ATLAS Sensitivity to FCNC top decays, ATL-PHYS-PUB-2005-009
25. J. Dodd et al., Study of ATLAS Sensitivity to Rare Top Quark Decays, ATL-PHYS-2003-016, May 1999
26. O. Çakır, S.A. Çetin, Anomalous single top quark production at the CERN LHC, SN-ATLAS-2004-046, August 2004
27. T. Sjöstrand et al., Comput. Phys. Commun. **135**, 238 (2001)
28. S.R. Slabospitsky, L. Sonnenschein, Comput. Phys. Commun. **148**, 87 (2002)
29. E. Richter-Was, D. Froidevaux, L. Poggioli, ATLFAST 2.0 – a fast simulation package for ATLAS, ATL-PHYS-98-138, November 1998
30. Athena – The ATLAS Common Framework, http://atlas-computing.web.cern.ch/ atlas-computing/documentation/ swDoc/ AthenaDeveloperGuide-8.0.0-draft.pdf
31. S. Eidelman et al., Phys. Lett. B **592**, 1 (2004)
32. DELPHI Collaboration, A.L. Read, DELPHI 97-158 PHYS 737 (1997)
33. A.L. Read, CERN report 2000-005 (2000) 81
34. L. Chikovani, T. Djobava, Study of ATLAS sensitivity to FCNC top quark decay $t \to Zq$, hep-ex/0008010, Aug. 2000
35. A. Juste, Top quark current experimental status, in proceeding of the TOP 2006: International Workshop on Top Quark Physics, PoS TOP2006:007,2006 (see presentation in http://nautilus.fis.uc.pt/personal/top2006/ programme.shtml)